VALIDATION OF *IN VITRO* MODELS FOR SMOKE EXPOSURE OF PRIMARY HUMAN BRONCHIAL EPITHELIAL CELLS

Michal Mastalerz[1], Elisabeth Dick[1], Ashesh Chakraborty[1], Elisabeth Hennen[1], Andrea C. Schamberger[1], Andreas Schröppel[1], Michael Lindner[2,3], Rudolf Hatz[4], Jürgen Behr[5], Anne Hilgendorff[1], Otmar Schmid[1], and Claudia A. Staab-Weijnitz[1*]

[1] *Institute of Lung Biology and Disease and Comprehensive Pneumology Center with the CPC-M bioArchive, Helmholtz Zentrum München, Member of the German Center for Lung Research (DZL), Munich, Germany*

[2] *Asklepios Fachkliniken München-Gauting, Munich, Germany*

[3] *Present address: University Department of Visceral and Thoracic Surgery Salzburg, Paracelsus Medical University, A-5020, Salzburg, Austria*

[4] *Thoraxchirurgisches Zentrum, Klinik für Allgemeine, Viszeral-, Transplantations-, Gefäß- und Thoraxchirurgie, Klinikum Großhadern, Ludwig-Maximilians-Universität (LMU), Munich, Germany*

[5] *Medizinische Klinik und Poliklinik V, Klinikum der Ludwig-Maximilians-Universität (LMU), Munich, Germany, Member of the German Center for Lung Research (DZL)*

[*]To whom correspondence should be addressed:

Claudia Staab-Weijnitz, Comprehensive Pneumology Center, Ludwig-Maximilians-Universität and Helmholtz Zentrum München, Max-Lebsche-Platz 31, 81377 München, Germany, Tel.: 0049(0)89-31874681; Fax: 0049(89)31874661; Email: staab-weijnitz@helmholtz-muenchen.de
ORCID-ID: https://orcid.org/0000-0002-1211-7834

Running title: Bronchial *in vitro* smoke exposure models

Keywords: Cigarette smoke, cigarette smoke extract, primary human bronchial epithelial cells, validation, *in vitro* smoke model, differentiation

Downloaded from journals.physiology.org/journal/ajplung at Helmholtz Zentrum Muenchen (146.107.008.161) on December 16, 2021.

Summary

Rationale. The bronchial epithelium is constantly challenged by inhalative insults including cigarette smoke (CS), a key risk factor for lung disease. *In vitro* exposure of bronchial epithelial cells using CS extract (CSE) is a widespread alternative to whole CS (wCS) exposure. However, CSE exposure protocols vary considerably between studies, precluding direct comparison of applied doses. Moreover, they are rarely validated in terms of physiological response *in vivo* and the relevance of the findings is often unclear. **Methods.** We tested six different exposure settings in primary human bronchial epithelial cells (phBECs), including five CSE protocols in comparison with wCS exposure. We quantified cell-delivered dose and directly compared all exposures using expression analysis of 10 well-established smoke-induced genes in bronchial epithelial cells. CSE exposure of phBECs was varied in terms of differentiation state, exposure route, duration of exposure, and dose. Gene expression was assessed by quantitative Real-Time PCR (qPCR) and Western Blot analysis. Cell type-specific expression of smoke-induced genes was analyzed by immunofluorescent analysis. **Results.** Three surprisingly dissimilar exposure types, namely chronic CSE treatment of differentiating phBECs, acute CSE treatment of submerged basal phBECs, and wCS exposure of differentiated phBECs performed best, resulting in significant upregulation of seven (chronic CSE) and six (acute wCS, acute submerged CSE exposure) out of 10 genes. Acute apical or basolateral exposure of differentiated phBECs with CSE was much less effective despite similar doses used. **Conclusions.** Our findings provide guidance for the design of human *in vitro* CS exposure models in experimental and translational lung research.

Downloaded from journals.physiology.org/journal/ajplung at Helmholtz Zentrum Muenchen (146.107.008.161) on December 16, 2021.

INTRODUCTION

Cigarette smoke (CS) contributes to 8 out of 10 most common causes of death, which consequently translates to 7 million deaths worldwide every year (1-3). The lung, as the most important portal of entry, develops a range of serious pathologies in response to CS, including chronic obstructive pulmonary disease (COPD) which currently is ranked fourth among the most common global causes of death (4). The bronchial epithelium provides the main first line of defense against inhaled insults like CS, which consists of thousands of compounds distributed among the gas and particle phase of the smoke (5). It is a pseudostratified layer of cells consisting of different cell types, the major ones being ciliated, club, goblet, and basal cells. Cell composition changes throughout the tracheobronchial tract. Mucus producing goblet cells and submucosal glands are more abundant in the trachea and upper respiratory tree whereas the lower airways are more populated by club cells (6). Each cell type serves specific functions in the maintenance of a physical barrier or detoxification of potentially harmful substances: Basal cells are the main airway progenitor cells, giving rise to all cell types in the conducting airway epithelium. Ciliated and goblet cells together form the mucociliary escalator, which is essential for the removal of harmful inhaled particles. Club cells secrete surfactant, have been ascribed a role in detoxification of xenobiotics, act as progenitor cells for ciliated and goblet cells (7) and have the ability to dedifferentiate into basal cells upon injury (8). Organization and structure of the bronchial epithelium can be drastically altered in chronic lung disease and it is known that CS contributes to squamous cell metaplasia, goblet cell hyperplasia, decrease of the ciliated cell population (9) and increased epithelial permeability (10).

Experimental settings to study the response of the airways to CS *in vitro* vary greatly in the literature. For instance, lung epithelial cells used for this purpose range from the use of immortalized or tumor-derived cell lines, such as A549 (11), BEAS-2B (12, 13) or NCI-H292 (14) to primary human bronchial epithelial cells (phBECs)(9, 15). Cells can further be cultured under submerged (16) conditions or at the air-liquid interface (ALI). For the latter, it becomes even more complex, as an ALI culture model can be exposed to CS components from the basolateral (9) or the apical side (17, 18). CS can also be delivered in different ways. Very frequently, a cigarette smoke extract (CSE) is used, which represents a rather straightforward and easily applicable technique (12, 19-21). In some studies cells were starved prior to exposure (16), or CSE was administered repeatedly over an extended period of time in efforts to mimic a chronic exposure (9). As for acute exposures, the duration varied from 30 min (14) up to 72 h (22). Also whole cigarette smoke (wCS) exposure is frequently applied (23-25) and considered to best mimic physiological CS delivery (24). This type of exposure, however, requires a more sophisticated exposure set-up not available to many experimental lung research laboratories, which is likely why many investigators resort to the use of CSE (12, 19-21).

Downloaded from journals.physiology.org/journal/ajplung at Helmholtz Zentrum Muenchen (146.107.008.161) on December 16, 2021.

A common limitation of such human *in vitro* studies is that typically little is done to standardize or validate experimental models using CS. With few exceptions where ISO and Canada health standardized protocols for smoking conditions and regimen ISO 3308:2012 (24, 25) were put in place, usually the choice of CSE concentration or delivered amount of CS was based on cytotoxicity assessments only, rarely on *CYP1A1* expression (9), or on blood levels of nicotine and other CS components in smokers (22). In addition, the delivered CS dose is rarely assessed which makes it inherently difficult to directly compare findings between different research laboratories, as even for a defined number of standard cigarettes the corresponding 100% CSE concentration depends on operational parameters such as a method of the whole smoke generation and amount of medium used. Finally, the experimental CSE exposure models have not been comprehensively assessed in terms of physiologically relevant gene expression changes, even though distinct transcriptomic signatures in current smokers relative to non-smokers are known (24, 26-31).

Here, based on the available literature, we selected five independent transcriptomic datasets, where gene expression in current smokers was compared to non-smokers, namely GSE994 (32), GSE4498 (33), GSE7895 (34), GSE20257 (35), and GSE52237 (36). Inclusion criteria for current smokers differed somewhat between these studies, but in four out of five studies current smokers were only included if they had no respiratory symptoms and normal pulmonary function tests: GSE994 (32), GSE20257 (35), GSE52237 (36) and GSE4498 (33). Beane and colleagues in GSE 7895 (34) excluded current smokers with lung cancer or unknown lung cancer status, but otherwise did not specify the respiratory health status of the smokers. From these five data sets, we carefully extracted a set of 10 genes, which we, for the purpose of this study, termed smoke exposure regulated genes (SERGs, Table 1). All SERGs were consistently significantly upregulated in all five data sets. Notably, we deliberately did not choose a combined set of the top 10 altered genes, but instead, included genes with very high (> 10; AKR1B10, CYP1A1, CYP1B1), high (> 5 and ≤ 10; ADH7, ALDH3A1, UCHL1) and moderate fold change (<5; AKR1C1, MUC5AC, NQO1, PIR, Table 1) in order to increase the dynamic range of our approach.

Here, we took advantage of these SERGs to standardize and validate different *in vitro* exposure models in terms of physiological response *in vivo*. For this comparison, we chose CSE exposure protocols and strategies typically used by the experimental lung research community and compared them with wCS exposure using a comparable dose. We tested acute exposure of submerged basal cells (21, 37, 38), acute basolateral (39) and acute apical exposure of differentiated phBECs (15, 40), here with and without prior starvation (16, 41, 42), and, finally, chronic basolateral exposure of differentiating cells at the ALI (9, 43). Even if basolateral exposure is much different from the physiological scenario, we have reported previously that this exposure model can recapitulate

Downloaded from journals.physiology.org/journal/ajplung at Helmholtz Zentrum Muenchen (146.107.008.161) on December 16, 2021.

smoke-induced changes like loss of barrier integrity and COPD-like changes in cell type composition (9). In addition, cell-delivered CS doses were quantified and compared to estimated doses of inhaled CS *in vivo*. Overall, we describe a novel strategy how *in vitro* cigarette smoke exposure models can be validated and standardized, which rests on two pillars: (1) Assessment of a physiologically highly relevant, human-derived gene expression signature for the smoking-induced response of the human airway, and (2) quantification of the cell-delivered dose facilitating the direct comparison of *in vitro* to *in vivo* doses received by smokers. This method was used to critically assess the physiological relevance of six acute and chronic *in vitro* models of smoking exposure of human primary bronchial cells, using cigarette smoke extract and whole smoke as current golden standards of cigarette smoke exposure.

Downloaded from journals.physiology.org/journal/ajplung at Helmholtz Zentrum Muenchen (146.107.008.161) on December 16, 2021.

MATERIALS AND METHODS

Patient material

Basal primary bronchial epithelial cells (phBECs) were obtained from either the CPC-M BioArchive at the Comprehensive Pneumology Center (CPC, six donors) or Lonza, Basel, Switzerland (three donors). PhBECs from the CPC-M BioArchive were derived from patients undergoing lung tumor resections and isolated from histologically normal regions adjacent to the resected lung tumors, who were either ex-smokers with a cessation period of >10 years or never smokers (Table S1), with similar size of small bronchi across donors. Upon treatment of bronchi with Pronase E, epithelial cells were carefully scraped with a scalpel, minced and filtered through a 70µm strainer to remove tissue pieces. To remove fibroblasts, cells were plated on uncoated plates for 3 hours. Afterwards, collected supernatant was transferred onto collagen I (C3867, Sigma Aldrich, Germany) coated plates and then cultured with PneumaCult™ Ex-Plus (Stemcell Technologies, 05041, Vancouver, Canada) with 1% Pen/Strep. Cells were expanded in passage 1 and then moved to liquid nitrogen storage until later use. PhBECs obtained from Lonza had been isolated from healthy self-reported non-smokers (2 females, 49 and 52 years old, and one 13 year old male). After isolation, all samples tested negative for *Mycoplasma pneumonia,* were expanded to passage 1, collected in freezing medium, and finally moved to liquid nitrogen storage until later use. All participants had given written informed consent, and the study was approved by the local ethics committee (454-12) of the Ludwig-Maximilians University of Munich, Germany.

Preparation of CSE

The mainstream smoke of six filtered reference cigarettes 3R4F (Kentucky Tobacco Research and Development Center at the University of Kentucky; Lexington, KY) was bubbled through 100 ml ALI-medium (Stemcell Technologies, 05041, Vancouver, Canada) or BEBM™ (Lonza, CC-3170) without supplements. CSE generation was carried out at a flow rate of 0.3 l/min and the resulting medium considered as 100% CSE. CSE was then filtered through a 0.2 µm filter (Minisart; Sartorius Stedim Biotech), aliquoted and immediately stored at -80°C. For gravimetric analysis and CSE exposure, aliquots were later thawed and used immediately at the indicated concentrations.

Determination of dose by gravimetric analysis

200µl of media used in experiments and media exposed to a cigarette smoke as described above was pipetted on Whatman® quartz filters (Sigma Aldrich) and placed inside a sealed desiccator until completely dry. The weight of the filters was measured before and after medium application. The difference between CSE-free and 100% CSE medium yielded the CS dose in 200 µl 100% CSE and was used for dose calculations for all CSE exposures.

Downloaded from journals.physiology.org/journal/ajplung at Helmholtz Zentrum Muenchen (146.107.008.161) on December 16, 2021.

Primers and antibodies

Primers were obtained from Eurofins Genomics Germany GmbH (Ebersberg, Germany) and are listed in Supplementary Table S2;. Supplementary Tables S3 and S4 contain the primary and secondary antibodies used in this study, respectively.

Primary bronchial epithelial cell cultivation and differentiation

For expansion, cells derived from BioArchive and Lonza were thawed at passage 1 and seeded at a density of 20,000-25,000 cells/cm^2 on 100 mm plates (Corning, 430167, New York, USA) using BEGM Bronchial Epithelial Cell Growth Medium BulletKit (Lonza CC-3170, containing: BEBM™ Clonetics Medium (CC-3170) + SingleQuots Supplements and Growth Factors (CC-4175)) + 100U Pen/Strep (Life Technologies, 10,000 U, 15140) or PneumaCult™ Ex-Plus (Stemcell Technologies, 05041, Vancouver, Canada) with 1% Pen/Strep. BEGM was used for expansion and acute submerged exposure of basal cells, in agreement with our previous studies (21, 44). In contrast, for all exposure types involving differentiation or differentiated cells, cells were expanded in PneumaCult™ Ex-Plus before differentiation at ALI. Upon reaching 80-90% confluency, cells were seeded on 12-well transwells (Corning, 3460, 12mm inserts, Polystyrene, 12-well plate, 0.4µm Polyester Membrane, Tissue Culture Treated, 1.12cm^2/transwell), coated with collagen IV (C7521, Sigma Aldrich, Germany) seeding 100,000 cells per membrane. The cells were air-lifted after reaching 100% confluency in 1-3 days and medium was changed to ALI-medium (PneumaCult™-ALI Medium, Stemcell Technologies, 05002 with added supplement (05003) and additives (05006)) and left for differentiation at the air-liquid interface for 28 days, with media changed every 2 days. Throughout the experiments, cells were cultured at 37°C in a humidified cell incubator with 95% air and 5% CO_2.

Transepithelial Electrical Resistance (TEER) Measurements

After adding apically pre-warmed HBSS (Lonza, CC-5024) onto inserts, cells were left to equilibrate at room temperature for at least 10 min. The TEER measurements were performed in triplicates for each insert, using a Millicell-ERS-2 volt-ohm-meter (Millipore, Billerica, MA) with a STX01 chopstick electrode (Millipore). For all treatment conditions, at least three individual wells per donor were analyzed. After measurement, the blank value (a similar measurement of a cell-free insert) was subtracted and the resulting value multiplied by the well surface area (1.12 cm^2 for 12-well transwell inserts from Corning) to yield Ω x cm^2.

Cigarette smoke exposure models

All cigarette smoke exposure models were performed in four to five independent experiments using phBECs derived from independent donors from the CPC BioArchive. In total, cells from six donors

Downloaded from journals.physiology.org/journal/ajplung at Helmholtz Zentrum Muenchen (146.107.008.161) on December 16, 2021.

were used and there was an overlap of at least three donors in all exposure models (Supplemental Table S1). Lonza cells were only used in addition for submerged acute basal cell exposure, taking advantage of samples already available from our previous study (21).

Acute submerged exposure of basal cells with CSE

Acute submerged exposure of basal cells with CSE was done as described previously (21). Briefly, after reaching 80%-90% confluency on a 100 mm dish cultured in BEGM, cells were washed in HBSS (Lonza, CC-5024) and then trypsinized using Trypsin with EDTA (Lonza, CC-5012). Reaction was stopped by Trypsin inhibitor TNS (Lonza, CC-5002). PhBECs were then centrifuged at 400 *g* for 5 min, the supernatant carefully removed and the cell pellet resuspended in BEGM medium, followed by counting in a CASY cell counter (OLS-OMNI Life Science, Bremen, Germany). The cells were then seeded on 6-well plates (TRP, 92406, 9,6cm^2/well) at a density of 1.0 x 10^4 cells/cm^2, cultured 3 days until confluency, and finally exposed to the indicated CSE concentrations for 24 h. Prior to mRNA or protein extraction, cells were washed twice with ice-cold HBSS and stored at -80°C.

Chronic and acute basolateral exposure with CSE

PhBECs were expanded in PneumaCult^{TM} Ex-Plus Medium on 100 mm dishes and subsequently seeded on 12-well transwell plates. Upon reaching 100% confluency in the inserts, cells were air-lifted (= day 0) and the basolateral medium was immediately changed to either ALI or 5% CSE in PneumaCult^{TM}-ALI medium, as described in (9). During the full differentiation period of four weeks, 5% CSE or PneumaCult^{TM}-ALI medium was regularly exchanged every two days. Every 7 days from airlift until day 28, inserts were either collected and stored in -80°C, or fixed in PFA for immunofluorescent (IF) analysis.

Acute basolateral CSE exposure was carried out on differentiated phBECs on day 28 after airlift. Here, cells were exposed to 5% CSE in the basolateral part for 24 h, after which cells were washed twice in ice-cold HBSS and stored at -80°C.

Acute apical exposure with CSE

Fully differentiated phBECs were treated for 24 h with 200µl of 3%, 6% or 12% of CSE from the apical side, followed by subsequent collection of cells, apical washes and media. In the experiment including starvation, cells were starved in PneumaCult^{TM}-ALI medium without supplements 24 h prior to the treatment, followed by the identical exposure and collection, as described above. As a control, a mock exposure with only PneumaCult^{TM}-ALI was used.

Downloaded from journals.physiology.org/journal/ajplung at Helmholtz Zentrum Muenchen (146.107.008.161) on December 16, 2021.

For direct comparison with exposure to whole cigarette smoke (see below), cells were treated 5 min with 200µl of 40% CSE added apically, followed by careful removal of the CSE without washing with HBSS, and incubation for 24 h at 37°C. Subsequently, cells were washed twice with ice cold HBSS and then stored at -80°C, along with apical washes and basolateral medium.

Air-Liquid Interface Cell Exposure with Whole Cigarette Smoke (ALICE-Smoke)

Transwell inserts with and without fully differentiated phBECs were put into the pre-warmed 12-well plate in the ALICE-Smoke chamber which is a 12-well insert adapted version of the stagnation flow system described preciously (45, 46). For dosimetry three to four 1.1 cm^2 metal plates were placed on three to four cell-free inserts. Then, 800 µl of pre-warmed PneumaCult™-ALI medium was added to the basolateral side of the transwell inserts. After tight assembly of the pre-warmed smoke chamber (Supplementary Figure S1; all Supplemental material is available at https://figshare.com/s/35a9228cd52d702ef622), it was placed into an incubation chamber (37°C) and inserts were exposed to a continuous flow of cigarette smoke, generated by burning 3 cm of filtered Research-grade cigarettes at a total flow rate of 0.6 L/min for about 2 min (0.05 L/min per transwell), followed by exposure to sterilized air for further 2 min. To measure the cell-delivered dose, the metal plates located in the inserts during exposure were collected in Falcon tubes and the deposited smoke components were dissolved in 1 ml absolute ethanol. Also the quartz filter located just downstream of the 12-well plate, which collects all of the smoke not deposited in the exposure chamber (>95% of total smoke (45, 47); Supplementary Figure S1), was placed in tightly closed plastic container with silica gel, dried for 2 h at room temperature, and weighed before and after exposure using an analytical balance to obtain the total smoke mass on the filter (M_{tot}). Next, the cigarette smoke components on the quartz filter were dissolved in 20 ml of absolute ethanol and the resulting solution with a known smoke concentration (M_{tot} /20 ml) was diluted 1:50. The cell-delivered cigarette smoke dose was determined by quantitative fluorescence analysis of all alcohol extracts (λ_{exc} 355 nm, λ_{em} 460 nm; Safire II Plate reader, Tecan, Männedorf, Switzerland). Measurements were carried out on Greiner 96-well microplate (Sigma-Aldrich, 655101, St. Luis, USA) in four technical replicates, using 99 % ethanol as a blank. Finally, based on the known weight and fluorescence of the deposited smoke dose on the outlet quartz filter, the dose deposited on each metal plate was calculated from the fluorescence intensity of the corresponding alcohol extract.

RNA Isolation and Real-Time Quantitative Reverse-Transcriptase PCR (qRT-PCR) Analysis

For RNA extraction from phBECs, the RNeasy Mini Plus Kit (Qiagen, 74136, Venlo, Netherlands) was used according to the manufacturer's instructions. RNA concentration was determined measuring absorbance in a NanoDrop 1000 spectrophotometer (NanoDrop Tech. Inc; Wilmington, Germany) at

Downloaded from journals.physiology.org/journal/ajplung at Helmholtz Zentrum Muenchen (146.107.008.161) on December 16, 2021.

260 nm. Next, RNA was reverse transcribed to cDNA using reverse transcriptase (Applied Biosystems, N8080018, Waltham, USA or Invitrogen, 28025013) and random hexamer primers (Applied Biosystems). For this, 1 µg RNA was diluted up to 20 µl with DNase/RNase free water, denatured at 70°C for 10 min and then incubated on ice for 5 min. 20 µl of cDNA synthesis master mix (5 mM MgCl2, 1x PCR buffer II (10x), 1 mM dGTP, 1 mM dATP, 1 mM dTTP, 1 mM dCTP, 1 U/µl RNase inhibitor, and 2.5 U/µl MuLV reverse transcriptase) was added to each sample and cDNA synthesis was performed for 60 min at 37°C, followed by 10 min incubation at 75°C. cDNA was diluted up to 200 µl with DNase/RNase-free water for usage in qRT-PCR analysis. qRT-PCR was performed in 96-well format using a Light Cycler® LC480II instrument (Roche) and LightCycler® 480 DNA SYBR Green I Master (Roche). Fold changes relative to control were calculated as $2^{-\Delta\Delta Ct}$ with $\Delta\Delta C_t = \Delta C_t$ (exposure) - ΔC_t (mock), where $\Delta Ct = C_t$ (gene of interest) – C_t (reference) for each condition. For specific gene amplification, primers listed in Supplementary Table S2 were used. For each exposure type, the most stable internal reference gene out of four (DHX8, WDR89, GADPH or HPRT) was determined and then used for standardization of relative mRNA expression. Gene expression changes were always similar for two independent internal reference genes. All qRT-PCR reactions were performed in technical duplicates and non-template controls were included for quality control.

Protein Isolation, SDS-Polyacrylamide Gel Electrophoresis (SDS-PAGE) and Immunoblotting

For protein isolation, cells were placed on ice, washed twice in ice-cold HBSS and scraped into 80 µl RIPA buffer (50 mM Tris•HCl, pH 7.6, 150 mM NaCl, 1% Nonidet P-40, 0.5% sodium deoxycholate, and 0.1% SDS) with Complete™ protease inhibitor cocktail (05892970001, Roche, Basel, Switzerland) and PhosSTOP™ phosphatase inhibitor cocktail (PHOSS-RO, Roche) with either a cell scratcher or a 1 ml pipette tip. The wells or inserts were washed once with an equal amount of RIPA buffer and transferred to the same tube. After incubation on ice for 30 min, tubes were centrifuged at 4 ^{o}C for 15 min at 14,000 RPM. Supernatants were collected and stored at -80^{0}C. Protein concentration was determined using the Pierce™ BCA Protein Assay Kit (23225, Thermo Scientific, Rockford, USA) according to manufacturer's instructions.

For SDS-PAGE, samples were denatured with Laemmli buffer (65 mM Tris-HCl pH 6.8, 10% glycerol, 2% SDS, 0.01% bromophenol blue, 100 mM DTT) and separated on 10% or 12% polyacrylamide gels. Proteins were transferred to polyvinylidene difluoride (PVDF) membranes (Thermo Scientific, 88518, Rockford, USA) using a wet tank blotting system (Mini PROTEAN® Tetra Cell, 552BR, Bio-Rad, Munich, Germany). After blocking for at least 30 min in 5% skimmed milk in TBS-T (0.1% Tween 20, TBS), membranes were washed three times for 10 minutes in TBS-T and incubated with primary antibody (see Supplementary Table S3) overnight at 4 ^{o}C. After washing three times for 10 min in TBS-T, membranes were incubated at room temperature with secondary antibodies (see Supplementary

Downloaded from journals.physiology.org/journal/ajplung at Helmholtz Zentrum Muenchen (146.107.008.161) on December 16, 2021.

Table S4), followed by visualization with SuperSignal™ West Pico, SuperSignal™ West Dura or SuperSignal™ West Femto Maximum Sensitivity Substrate, according to the intensity of the detected signals (all Thermo Fisher Scientific, 34079, 37071, 34095, respectively) and analyzed by the ChemiDocXRS+ imaging system (Bio-Rad, Munich, Germany).

Cytotoxicity Assay

After each exposure, the apical and basolateral supernatants were collected and stored at -80 ^{o}C. After preparing high control by lysing cells in 2% Triton-X/media/0% FCS, the supernatants were centrifuged at 250 *g* for 10 min. The supernatants in each tube were carefully collected and then 30 µl of the supernatants were pipetted into a Greiner 96-well microplate (Sigma-Aldrich), followed by quantification of lactate dehydrogenase (LDH) release using the cytotoxicity detection kit (LDH , 11644793001, Sigma-Aldrich) according to manufacturer's instructions.

Immunofluorescence Analysis

PhBECs were stained on the transwell membrane and the different cell types quantified as described previously (44). Following the indicated treatment, phBECs were washed twice in HBSS and fixed from the apical and basolateral side with 3.7% paraformaldehyde (PFA) overnight at 4 ^{o}C or 1 h at room temperature. After aspirating PFA, the inserts were washed in 1x PBS and then either stored at 4 ^{o}C until usage or immediately permeabilized with 0.2% Triton X-100/PBS for 5 min. The inserts were then again washed with PBS and blocked with 5% BSA/0.2% Tween/PBS for 1 h at room temperature. PhBECs were stained directly on the transwell membrane after cutting into quarters or six pieces using a scalpel. Membrane fragments were transferred to a 24-well plate and the appropriate primary antibody was applied (see Supplementary Table S3), diluted in 5% BSA/0.2% Tween/PBS for 1h at room temperature or overnight at 4°C (volume: 150 µl). Afterwards, membranes were washed three times with PBS for 5 min. Then, the secondary antibody conjugated with either Alexa Fluor 488 or Alexa Fluor 568 (see Supplementary Table S4) diluted in the same buffer was applied and incubated for 30 min at room temperature protected from light by aluminum foil. Nuclei were stained with 0.5 µg/ml 4,6-diamidino-2-phenylindole (DAPI) at 1:2000 dilution. Membranes were again washed three times in PBS, mounted in fluorescent mounting medium (Dako, S3023, Hamburg, Germany) and dried overnight at room temperature. Fluorescent microscopy was performed using an upright microscope (Axiovert II; Carl Zeiss AG; Oberkochen, Germany). Images were processed using ZEN 2010 software (Carl Zeiss AG) or Imaris 7.4.0 software (Bitplane; Zurich, Switzerland). Immunofluorescence quantification was performed using Imaris 7.4.0 software (Bitplane). For this, z-stack images of stained transwell membranes were obtained by fluorescent microscopy and 1500 –

Downloaded from journals.physiology.org/journal/ajplung at Helmholtz Zentrum Muenchen (146.107.008.161) on December 16, 2021.

4500 cells per image were analyzed for positivity of specific markers, largely as described previously (9).

Downloaded from journals.physiology.org/journal/ajplung at Helmholtz Zentrum Muenchen (146.107.008.161) on December 16, 2021.

Statistical Analysis

Results are depicted as mean ± SD and derived from at least four independent experiments, where each experiment was performed with cells from a different donor. All data sets were tested for normal Gaussian distribution using the Shapiro-Wilk test. Data distribution was normal for all experiments with single comparisons, *i.e.* wCS, acute apical 40% CSE, and basolateral acute 5% CSE exposure. For these, we used a paired, two tailed student's *t*-test. Distribution of a few data sets in submerged basal CSE, acute apical CSE, and basolateral chronic CSE exposure was not normal. However, as tests for normal distribution are insensitive to small sample sizes, we nevertheless used parametric test methods, which are more suitable for very small sample sizes, accepting the risk that the assumption of normal distribution may not be met in all cases. Accordingly, repeated measures ANOVA with Bonferroni correction was used for all multiple comparisons. Notably, using non-parametric testing for the few data sets, which were not normally distributed (Friedman test with Dunn's correction), did not change the overall results: Statistical significance was reached for the same genes, albeit with higher p-values reflecting the lower statistical power of the non-parametric test.

For comparing baseline expression of AhR-responsive SERGs (supplemental Figure S2) a non-parametric Friedman test with Dunn's correction was used, while significance between donors in baseline expression levels of SERGs (supplemental Figure S3) was tested by using one-way ANOVA with Bonferroni correction. CSE gravimetric measurements (supplemental Figure S4) significance was assessed by using unpaired two tailed student's *t*-test. This information is also given in the figure legend and where applicable. All statistical calculations were carried out in GraphPad Prism 8 Software (San Francisco, CA). Significance levels: *$p<0.05$, **$p<0.01$, ***$p<0.001$ ****$p<0.0001$.

Downloaded from journals.physiology.org/journal/ajplung at Helmholtz Zentrum Muenchen (146.107.008.161) on December 16, 2021.

RESULTS

Quantitative analysis of cigarette smoke mass allows for direct dose comparisons between different experimental models

To facilitate comparison of cell-delivered dose between CS exposure models, the mass of cigarette smoke contained in CSE and the smoke mass deposited on the cells during whole smoke exposure were experimentally determined. Briefly, 200 µl of 100% CSE and CSE-free medium were pipetted onto separate quartz filters, and, after complete drying, the CSE mass was determined by gravimetric analysis. CSE was generated in two different media using identical settings described above, resulting in very similar CSE concentrations (PneumaCult™-ALI medium: 1.40 mg/ml; BEGM medium: 1.25 mg/ml) (Supplementary Figure S4). From the known dilution of CSE in and the volume of cell culture medium supplied to the cells, the mass of CSE per exposed cell area could be calculated for each CSE exposure scenario.

For determining the mass of whole CS deposited on each insert in the ALICE-Smoke system, metal plates were placed in unoccupied inserts and a gravimetrically known mass of whole CS was collected on a quartz filter downstream of the ALICE-Smoke exposure chamber. After performing quantitative spectrofluorometry on alcohol extracts from both the plates and the filter, the mass dose in all CSE exposure models could be calculated as the total mass of cigarette smoke applied per area of the exposed cell layer area (Table 2).

Differentiation of phBECs was successful

Immunofluorescent stainings for p63, acetylated tubulin, CC10 and MUC5AC at day 0, 7, 14, 21 and 28 of differentiation showed successful generation of all major cell types at the expense of basal cells, with percentages that resemble the physiological cell type composition in larger airways (48-50) (Figure 1 B, C). TEER is a measure of cell adhesion and epithelial cell junctions' integrity (51). Weekly measurements demonstrated the establishment of an intact epithelial barrier early during the differentiation procedure (Figure 1D). TEER showed considerable donor variability, in particular at early time points, while levels were highly consistent after 4 weeks of differentiation. The immunofluorescence pictures, along with quantification of cell types indicate differentiation of basal cells into a full-blown bronchial epithelium with all main cell types.

Cells were exposed to non-toxic doses of cigarette smoke

In order to evaluate cytotoxic effects of CS, LDH and TEER measurements were carried out following each exposure. The post-exposure LDH release and TEER values were not significantly different from the controls for whole cigarette smoke (wCS, ALICE-Smoke) and apical CSE exposure (Supplementary

Downloaded from journals.physiology.org/journal/ajplung at Helmholtz Zentrum Muenchen (146.107.008.161) on December 16, 2021.

Figure S5), while basolateral exposure with the same CSE concentrations has been established as non-toxic previously, both for basal phBECs and fully differentiated phBECs (9, 21, 44). Both TEER and LDH data showed that phBECs were exposed to non-toxic doses of smoke.

Response of phBECs to CS strongly depends on exposure type and cell composition

In total, six different CS exposure settings were evaluated in terms of expression of 10 smoke exposure regulated genes (SERGs) (Table 1). Notably, for all of these exposures we used phBECs from at least four donors isolated under standardized conditions from the same source (Table S1). Of these, the following three settings were comparably effective in upregulation of SERGs on transcript level: Submerged acute exposure of basal cells with CSE upregulated six SERGs (*AKR1B10*, *AKR1C1, CYP1A1, NQO1, PIR, UCHL1*); chronic basolateral exposure with CSE during the complete period of differentiation upregulated seven SERGs (*AKR1B10*, *AKR1C1*, *ALDH3A1, CYP1A1, CYP1B1, NQO1, PIR)*; and ALICE-Smoke CS exposure upregulated six SERGs (*AKR1B10*, *AKR1C1, CYP1A1, CYP1B1, NQO1, UCHL1*). In contrast, acute apical and basolateral exposure to various concentrations of CSE did not alter the expression of more than one gene (Table 3). The specific results are described in more detail in the following.

Submerged exposure of basal cells with CSE upregulates six out of nine possible SERGs

One SERG, MUC5AC, is a goblet cell specific protein and was thus, as expected, not expressed by basal cells (data not shown). Out of the remaining nine SERGs, qRT-PCR analysis demonstrated significant upregulation of six (*AKR1B10*, *AKR1C1, CYP1A1, NQO1, PIR, UCHL1*), when undifferentiated basal cells were exposed to CSE under submerged conditions (Figure 2A, B). Upregulation was dose-dependent for AKR1B10, UCHL1, NQO1, AKR1C1 and PIR, but not for CYP1A1. Unexpectedly, ADH7 transcript levels were significantly reduced. In addition, we took advantage of samples from previously performed experiments (21) with cells purchased from Lonza (Supplementary Figure S6, n=3), where we even observed upregulation of all SERGs except for ADH7 which again was significantly and dose-dependently reduced in those cells. This demonstrates that upregulation of SERGs in this model is a robust finding, independent of cell sources. The results from all seven donors were not pooled in order to provide better comparability between the models, as the commercially available cells had only been used for this exposure setting. For selected SERGs, we also assessed regulation on the protein level. Similar to the transcript data, we observed a dose-dependent increase of AKR1B10, AKR1C1, and NQO1 protein (Figure 2C). Also ALDH3A1 protein was upregulated in a dose-dependent manner in all three experiments, unlike to what we observed on transcript level (Figure 2B and C). In contrast, the commercially available cells failed to upregulate

Downloaded from journals.physiology.org/journal/ajplung at Helmholtz Zentrum Muenchen (146.107.008.161) on December 16, 2021.

ALDH3A1 on protein level, even though upregulation of ALDH3A1 was significant on transcript level (Supplementary Figure S6).

Chronic basolateral exposure with CSE during differentiation upregulates seven out of ten SERGs

Here, cells were continuously treated with 5% CSE basolaterally for 28 days, *i.e.* throughout the entire differentiation, similar to the set-up used in Schamberger *et al* (9) (Figure 3A). The treatment resulted in trends for lower TEER values (Figure S7A), increased basal cell populations and decreased number of ciliated cells, all of which, however, failed to reach significance (Figure S7B). In contrast to our previous findings, numbers of goblet and club cells were not affected by 5% CSE. The RT-qPCR analysis demonstrated significant upregulation of seven out of 10 SERGs (*AKR1B10*, *AKR1C1, ALDH3A1, CYP1A1, CYP1B1, NQO1, PIR,* Figure 3B). Upregulation of CYP1B1 and CYP1A1 was dramatic (up to and more than 10-fold, respectively) in comparison to the remaining SERGs with moderate fold changes around +2. Upregulation of AKR1B10, NQO1 and ALDH3A1 was confirmed on protein level by Western blot analysis (Figure 3C).

Exposure with whole cigarette smoke (wCS) upregulates six out of ten SERGs, but with markedly higher fold changes

Here, in efforts to better mimic physiological exposure, fully differentiated phBECs were exposed to wCS using the ALICE-Smoke device (Figure 4A, Supplementary Figure S1). Expression of six out of 10 SERGs was significantly upregulated (*AKR1B10, AKR1C1, CYP1A1, CYP1B1, NQO1, UCHL1*, Figure 4B) and confirmed on protein level for AKR1B10, AKR1C1, and NQO1 (Figure 4C). Similar to the transcript data, ALDH3A1 was not consistently upregulated on protein level either. Notably, for *CYP1A1*, *CYP1B1* and *UCHL1*, the observed upregulation fold changes were by magnitudes higher than in the other exposure models. Also *AKR1B10* and *AKR1C1* were upregulated more than 5-fold, while *NQO1* showed similar upregulation as in the above described exposure models. Unexpectedly, expression of *MUC5AC* was significantly downregulated.

Acute CSE exposures on differentiated cells have substantially lower influence on SERGs

As the ALICE-Smoke system allows for quantification of the cell-delivered CS dose per area of exposed cell layer (µg/cm^2), we additionally performed an experiment where we exposed the cells in parallel experiments from the apical side to a high non-toxic dose of CSE. Based on the gravimetric measurements (Supplementary Figure S4), 40% CSE corresponded to a dose of 100 µg/ cm^2, which was about 8 times higher than the determined CS deposition by wCS (12±1.5 µg/cm^2). CSE was applied for 5 min, similar to the time wCS was applied in ALICE-Smoke. Notably, in sharp contrast to

Downloaded from journals.physiology.org/journal/ajplung at Helmholtz Zentrum Muenchen (146.107.008.161) on December 16, 2021.

the exposure by direct smoke, this exposure type failed to upregulate any of the reference genes (Figure 4).

Apart from this direct comparison with wCS, apical CSE exposures were also assessed in other settings: Acute apical exposure (Figure 5A) using 3%, 6% and 12% CSE for 24 h corresponded to CS doses of 7.5, 15 and 30 µg/cm^2, very similar to the 12µg/cm^2 determined for wCS. Here, only *CYP1A1* was significantly upregulated (Figure 5B), and starvation prior to exposure did not increase the number of upregulated SERGs, also only resulting in significant upregulation of *CYP1A1* (Supplementary Figure S8).

CSE was applied in acute manner also basolaterally, where cells were treated with 5% CSE for 24 h (Figure 6A). In contrast to chronic treatment, here only *CYP1A1* was significantly upregulated, similarly to the 24 h apical treatments (Figure 6B). Negative results for ALDH3A1, AKR1B10, AKR1C1 and NQO1 were confirmed on protein level (Figure 6C).

Immunofluorescence analysis shows expression of SERGs by basal and luminal cell types

As exposure of basal cells alone had resulted in induction of as many SERGs as wCS exposure, we hypothesized that basal cells are the main expressers of SERGs. To address this question in a model, which features a substantial smoke response and contains all major cell types, we chose wCS exposure and assessed colocalization of 4 selected SERGs (AKR1C1, NQO1, PIR and UCHL1) with markers of all major bronchial cell types. As expected, immunofluorescence analysis revealed upregulation of SERG-positive cells upon wCS exposure (Figure 4D). Moreover, all 4 SERG proteins assessed showed some colocalization with p63, a specific marker for basal cells (Figure 7). Nevertheless, NQO1, PIR and UCHL1 were mostly expressed by ciliated cells, as judged from colocalisation with acetylated tubulin (acTub, Figure 7, Supplementary Figure S9). In contrast, AKR1C1 colocalized mostly with the club cell-specific marker CC10 and not with the ciliated cell marker acTub. Very little colocalization was observed for the selected SERGs with MUC5AC, the marker for goblet cells.

Downloaded from journals.physiology.org/journal/ajplung at Helmholtz Zentrum Muenchen (146.107.008.161) on December 16, 2021.

DISCUSSION

In the present study, we defined a set of smoke-related reference genes (the SERGs, Table 1), based on known expression changes in current versus non-smokers, for validation of the physiological relevance of human *in vitro* smoke exposure models. Using phBECs, we assessed SERG expression in six different cigarette smoke exposure models (Table 2): (1) Acute submerged basal cell CSE exposure (Figure 2), (2) chronic basolateral exposure of differentiating phBECs with CSE (Figure 3), (3) acute apical exposure of differentiated phBECs with CSE (Figure 5 and Supplementary Figure S8), (4) acute basolateral exposure of differentiated phBECs with CSE (Figure 6), (5) and short acute apical exposure of differentiated phBECs with CSE in direct comparison with (6) apical exposure to wCS (Figure 4). No *in vitro* exposure model resulted in upregulation of all 10 SERG, but three surprisingly dissimilar exposure types, namely acute CSE treatment of basal submerged phBECs, chronic CSE treatment of differentiating phBECs, and wCS exposure of differentiated phBECs were similarly effective, upregulating six to seven SERGs. The other three CS exposure models were much less representative of the clinically observed gene regulation profile (<2 out of 10 SERGs) in spite of similar cell-delivered doses of CS used.

The current state-of-the-art of CS exposure, wCS, is available to few laboratories worldwide, which is why many investigators in experimental and translational lung research resort to simpler exposure settings as *e.g.* the use of CSE (12, 19-21). The preparation of CSE typically involves passing cigarette smoke through medium, where neither the number of cigarettes smoked nor the volume of medium used to capture the smoke nor the cigarette smoking regiment are standardized. Consequently, the generated 100 % CSE is not consistent throughout the literature (9, 52-54). On the other hand, when using whole cigarette smoke directly on cells, the dose of deposited cigarette smoke particulates typically remains unknown (55, 56) or is selected based on cell viability with unknown physiological relevance (57).

Here, we were able to experimentally determine the cell-delivered CS dose for both CSE and wCS exposure scenarios. This allowed not only for direct comparison of doses between different exposure settings, but also for an estimation how physiologically relevant the used dose is relative to *in vivo* exposure. For instance, it is known that approximately 82% of the inhaled smoke mass deposits on the 70 – 140 m^2 of lung epithelium (58, 59), and that the inhaled CS mass per smoked cigarette is about 10 mg (60). Notably, due to the physical properties of the bronchial airways, the impact of CS varies dependent on location in the bronchial tree and the main sites of CS particle deposition correlate with manifestation of lung diseases, such as lung cancer (61-63). Higher doses are possible at the airways' carinas of bifurcation, where the deposition can be increased up to 100-fold (64). Taken together, the theoretical maximal cigarette smoke (CS) mass per surface area and per cigarette

Downloaded from journals.physiology.org/journal/ajplung at Helmholtz Zentrum Muenchen (146.107.008.161) on December 16, 2021.

may thus be within the range of 0.59 – 1.17 µg/cm^2 in areas of high exposure like the aforementioned carinas of bifurcations. The CS doses we used in our exposure models (6 – 100 µg/cm^2) were ca. 10 to 100-fold larger than the expected hot spot dose a smoker receives after smoking one cigarette (Table 2). It corresponds to the cumulative dose from 10 – 100 cigarettes. In many cases this represents the daily CS dose of a smoker, justifying the 24 h of incubation time chosen here for most of the *in vitro* experiments. In the direct comparison between CSE and wCS, an incubation time of 5 minutes with CSE was used (Figure 4). This was done in efforts to adapt an exposure duration similar to wCS exposure. Despite the fact that, here, the cells were intentionally not washed after aspiration of CSE, it is possible that they were not affected by the total dose of CSE applied due to the shorter exposure time on the one hand, but also due to possible scavenging of toxic compounds by free thiols or amines in the cell culture medium used to generate the CSE. However, the total dose was significantly higher (≈8-fold), so reasonable comparability may still be given for a fraction of the applied dose. In addition, wCS exposure can also directly be compared to apical CSE exposure for 24 h (Figure 5 and Supplementary Figure S8). In this case, however, air-liquid interface was compromised for the time of exposure, which is not a physiological scenario. Nevertheless, both systems had a strikingly lower effect on the cells as compared to wCS exposure.

The genetic expression profile of bronchial epithelial cells in current smokers varies greatly when compared to non-smokers (32-36). Here, we took advantage of this knowledge to test whether several human *in vitro* CS exposure models recapitulate smoke-induced expression changes *in vivo*. We carefully selected a set of 10 genes with substantial and consistent upregulation in smokers' epithelial cells (SERGS, Table 1) to validate various smoke exposure models (Table 2). The choice of CSE exposure models, which we directly compared to wCS exposure, was based on models widely used by the lung research community (9, 15, 16, 21, 65, 66). There were no significant differences in basal expression of all SERGs between never smokers and ex-smokers used in experiments (Figure S3).

The human bronchial epithelium is a pseudostratified layer of different cell types, which can be generated *in vitro* using primary bronchial epithelial cells cultured at the air-liquid interface. It is well established that cell type composition and gene expression can be dramatically altered by cigarette smoke, both *in vivo* (67, 68) and *in vitro* (9, 21, 65). However, to the best of our knowledge, no study has directly compared smoke-induced gene expression changes *in vivo* and *in vitro* in a more comprehensive manner. Previous studies, including our own, have used *CYP1A1* as a marker for the efficacy of CSE (9, 69) as *CYP1A1* expression is well known to be induced by polycyclic aromatic hydrocarbons (PAH) as *e.g.* benzo[a]pyrene and tetrachlorodibenzo-*p*-dioxin (TCDD), compounds which are highly abundant in cigarette smoke (70). This induction results from activation of the aryl

Downloaded from journals.physiology.org/journal/ajplung at Helmholtz Zentrum Muenchen (146.107.008.161) on December 16, 2021.

hydrocarbon (Ah) receptor which, after heterodimerization with the aryl hydrocarbon receptor nuclear translocator (ARNT) protein, binds to the xenobiotic responsive element (XRE) of the *CYP1A1* promoter and activates gene transcription (71). Notably, except for acute high-dose exposure with 40% CSE, all of our exposure models resulted in upregulation of *CYP1A1*, implying that *CYP1A1* induction is a robust indicator of exposure to CS components. However, at the same time it becomes apparent that *CYP1A1* induction is not representative for CS-induced gene regulation, as in two models it remained the only strongly affected gene of all 10 SERGs. Intriguingly, other SERGs known to be directly induced by canonical AhR signalling, namely *CYP1B1*, *NQO1*, and *ALDH3A1* (72, 73) were often not induced in parallel with *CYP1A1* and never with a similarly high fold change (Table 3). This may in part be due to different levels of constitutive expression because induction of genes with very low basal transcription may lead to much higher fold changes than induction of genes that show considerable basal expression. Indeed, basal *CYP1A1* expression in all exposure models was much lower than the other AhR-responsive SERGs *CYP1B1*, *NQO1*, and *ALDH3A1* (Supplementary Figure S2). However, this also indicates that mechanisms other than direct canonical AhR signalling are important in this context and that it therefore is not sufficient to rely on *CYP1A1* induction for validation of the efficacy of CS exposure.

Importantly, AhR signalling also leads to induction of nuclear factor erythroid 2 related factor 2 (Nrf2) (74), in turn a potent inducer of a battery of antioxidant proteins including the SERGs ADH7 (75, 76), AKR1B10 and AKR1C1 (77-79), ALDH3A1 (75), NQO1 (75, 80, 81), PIR (82) and probably also UCHL1 (83). With Nrf2 being an AhR target, Nrf2-mediated gene regulation is delayed, relative to the direct AhR response. In addition, CYP1A1 produces reactive oxygen species (ROS) during its catalytic cycle (84) which also leads to an induction of Nrf2 signalling (85). Consequently, high *CYP1A1* induction, as a biomarker for potent AhR activation as well as a direct inducer of oxidative stress, should lead to subsequent induction of almost all SERGs in our exposure models. While this is likely to be true for wCS exposure, our remaining data does not demonstrate such a clear relationship. For instance, acute basolateral and apical exposure with CSE for 24 h resulted in clear upregulation of *CYP1A1*, but none or only few of the Nrf2-responsive genes. At the same time, induction of *CYP1A1* in submerged basal cells upon CSE treatment was comparably moderate but accompanied by induction of several Nrf2 target genes (Table 3).

Surprisingly, two SERGs, namely MUC5AC and ADH7, were not upregulated in any of the exposure models. In fact, *ADH7* and *MUC5AC* transcription was either not altered or even significantly downregulated. In our previous work, we observed an increase of MUC5AC^{+} cells upon chronic basolateral exposure with 5 % CSE in phBECs, which, however, was also not accompanied by the corresponding change in transcript levels (9). In contrast, Di and colleagues found moderately

Downloaded from journals.physiology.org/journal/ajplung at Helmholtz Zentrum Muenchen (146.107.008.161) on December 16, 2021.

increased MUC5AC expression in response to CSE treatment (86). On the other hand, recent evidence even suggests that CSE exposure may downregulate *MUC5AC* expression via activation of Notch signalling in epithelial cells (87, 88). We speculate that components of the cell culture medium, optimized to sustain a fully differentiated bronchial epithelium, may mask some deleterious effects by CS. This could also be true for *ADH7*, which encodes class IV alcohol dehydrogenase, an enzyme known to be involved in retinol and first-pass ethanol metabolism in the gastric epithelium (89, 90). While little is known about regulation of *ADH7* itself, another retinol-oxidizing member of the alcohol dehydrogenase family, ADH1C (gene *ADH3*) is regulated by retinoic acid (91, 92), a typical component of bronchial epithelial cell media (93). Taken together, the components of commercially available media, allowing for optimal growth and maintenance of organotypic bronchial epithelia, are not disclosed and may mask some effects caused by inhaled toxins observed *in vivo*. Of note, it has been previously reported that the choice of medium can affect phBEC culture (94). Furthermore, the absence of an immune compartment and other minor bronchial epithelial cell types as *e.g.* tuft or neuroendocrine cells could also lead to discrepancies *in vivo* and *in vitro*. These clearly are limitations of all of our models.

According to our collective results, three surprisingly dissimilar exposure types, namely acute CSE treatment of basal submerged phBECs, chronic CSE treatment of differentiating phBECs, and wCS exposure of differentiated phBECs, were comparably effective in CS response when counting the number of significantly induced SERGs (six or seven out of 10 SERGs, Figures 2, 3 and 4, Table 3). Importantly, this assessment is based on transcript levels only, the same readout on which our selection of SERGs was based on. We also assessed expression of some SERGs on protein level and overall found similar trends for upregulation, albeit often not as pronounced as on transcript level. Similar expression changes can be found to some extent in the literature for both CSE (9) and wCS (56). Notably, with this study, we show that the two CS exposure models we have used in previous studies, exposure of basal cells with CSE (21, 65) and chronic basolateral exposure with CSE (9) are among the three best *in vitro* models assessed here. In qualitative agreement with our previous studies (9), we observed trends for a reduction of TEER, for an increased basal cell population, and for a reduction of ciliated cells in response to chronic basolateral exposure to 5% CSE. However, none of these changes reached statistical significance and we did not either observe an effect on goblet or club cells as we had reported earlier (9). We believe this to be caused by two changes in the current set-up compared to our previous studies. Firstly, for all experiments involving differentiating or differentiated cells, we used a different expansion medium, namely PneumaCult™ Ex-Plus (Stemcell) *versus* previously BEGM (Lonza). A recent report has highlighted that different differentiation media have a strong effect on structural and functional properties of the differentiated bronchial epithelium (95). While the differentiation medium in our studies remained the same, we speculate that also the

Downloaded from journals.physiology.org/journal/ajplung at Helmholtz Zentrum Muenchen (146.107.008.161) on December 16, 2021.

use of a different expansion medium may have persistent effects on the differentiating cultures. Secondly, we used different cell sources and a different number of biological replicates in these studies: While in the present study, phBECs were derived from histologically normal regions adjacent to lung tumors from non-smokers and ex-smokers and all five differentiations +/- CSE were performed with cells from independent donors, we had previously used commercial basal cells from Lonza, all from self-reported healthy non-smokers, and performed several independent differentiations from two biological replicates only. The approach used in the current study is associated with a considerable increase in biological variability, making it inherently more difficult to obtain statistically significant results.

Considering the amplitudes of gene expression changes, wCS exposure clearly represents the model with the highest sensitivity in acute responses (Figure 4, Table 3). But taken together, similar to wCS exposure, submerged basal cell and chronic exposure of differentiating cells to CSE can be proposed as models that also reasonably well recapitulate the most substantial gene expression changes seen in *in vivo* cigarette smoke exposure (Table 3). Regarding the general applicability of CS exposure models, wCS exposure requires a fairly sophisticated experimental set-up, which is not available to all research laboratories. In that case, submerged exposure of basal cells to CSE is a reasonably good and quick-and-easy-to-perform model, which does not require the use of differentiation media and long-term culture. For research questions that require the full cell type composition of a bronchial epithelium, chronic basolateral exposure may be the model of choice.

Interestingly, submerged basal cell exposure with CSE as well as chronic basolateral exposure, where again, in particular during the initial phase of differentiation, predominantly basal cells are in direct contact with the CSE-containing medium, were far more efficient in upregulating SERGs than apical and acute basolateral CSE exposure of fully differentiated phBECs. We therefore hypothesized that basal cells have a pivotal role in the response to cigarette smoke and express SERGs. Hence, we assessed the cellular localization of AKR1C1, NQO1, PIRIN and UCHL1 in fully differentiated cells, using the most sensitive model, wCS exposure (ALICE-Smoke). Indeed, basal cells did express all SERGs assessed, but contributed relatively little to their overall expression. In fact, NQO1, PIR and UCHL1 were predominantly expressed by ciliated cells (NQO1, PIRIN, UCHL1), and AKR1C1 by club cells (Figure 7). In line with our results, NQO1 has been previously reported to be overexpressed in ciliated cells, where it may protect the bronchial epithelium, in particular the basal progenitor cells, from inhaled toxic substances and carcinogens (96, 97). Similarly, expression in basal and ciliated cells has been described for UCHL1 (98), a hydrolase associated with ubiquitin homeostasis, degradation of proteins (99), and cell apoptosis (100). In contrast to our results, AKR1C1, an aldo-keto reductase responsible for breaking down toxic aldehydes widely present in tobacco smoke, has been reported

Downloaded from journals.physiology.org/journal/ajplung at Helmholtz Zentrum Muenchen (146.107.008.161) on December 16, 2021.

as expressed by ciliated cells and not club cells (31). Finally, the function of PIR in ciliated cells is less clear and its expression in ciliated cells has not been described previously.

As upregulation of SERGs in basal cells in the absence of other differentiated cell types was substantial, our results suggest that under certain conditions, basal cells are capable of xenobiotic metabolism and protection from oxidative stress. This may play an important role during bronchial epithelial injury for example, where, following luminal cell depletion, basal cells will be more exposed to inhaled toxic agents, but, as progenitor cells, indispensable for the necessary epithelial repair. Here, efficient upregulation of protection mechanisms against oxidative stress and mutagenic substances may be crucial for prevention of lung disease. In contrast, in an intact bronchial epithelium, basal cells may be protected from inhaled insults by club, ciliated and goblet cells, which, projecting into the lumen, provide the first-line defence.

A striking result of our study was that, in sharp contrast to wCS exposure, CSE failed to upregulate any of the SERGs when applied to fully differentiated phBECs, even at an eight-fold higher dose (Figure 4). We chose this considerably higher non-toxic CSE concentration for this experiment because, even if for soluble chemicals the administered dose in general provides a reasonably accurate estimate of cell-delivered dose (101), CS components in CSE may be less bioavailable for the cells than the directly surface-applied wCS, as they will in part be bound to scavengers in the medium (*e.g.* proteins, free thiols, free amines). Therefore, ultimately, our observation that a substantially higher CSE dose still does not induce SERG expression, is more informative than if we had used the exact same dose. The drastically different efficacy in SERG expression between CSE and wCS most likely reflects the different constitutions of CSE and wCS in terms of cigarette smoke components: the water soluble components of wCS, which are retained in CSE, correspond to less than 40% of total wCS mass (102). Also, AhR signalling, which underlies induction of most of the SERGs, either directly or indirectly via Nrf2 signalling, is induced by highly hydrophobic compounds, a large part of which may not be retained in CSE (103). In addition, as mentioned above, toxicants in CSE may be partly scavenged by media components. Furthermore, even though cytotoxicity measurements reported by others (104) and our own previous measurements of mitochondrial superoxide and oxidative potential (21) indicate that CSE retains potency after freezing at -80°C, the use of frozen instead of freshly produced CSE may have destroyed some of the active ingredients in CSE. Considering these discrepancies between CSE and wCS, it is again remarkable that basal cells alone are capable of strong upregulation of SERGs upon CSE treatment, even though the absolute concentration of PAH in CSE probably is relatively low, toxicants may be scavenged by media components, and freeze-thawing may have destroyed other active ingredients.

Downloaded from journals.physiology.org/journal/ajplung at Helmholtz Zentrum Muenchen (146.107.008.161) on December 16, 2021.

In conclusion, we have validated six different *in vitro* CS exposure settings of primary bronchial epithelial cells based on induction of carefully selected genes regulated by cigarette smoke exposure, collectively called SERGs, *in vivo*. Notably, quantification of CS dose for all exposure types allowed for dose-matched experiments applying comparable CS doses, and thus allowing for further standardization. Among these models, three quite dissimilar exposure types performed best: chronic basolateral CSE treatment of differentiating phBECs significantly induced seven out of 10 SERGs, while acute CSE treatment of basal submerged phBECs and wCS exposure of differentiated phBECs significantly induced six out of 10 SERGs. Notably, acute CSE exposure of differentiated cells was ineffective, independent whether CSE was applied basolaterally or apically. Our results emphasize the need for validation of CS exposure models beyond assessment of viability and expression of the classical AhR-induced gene *CYP1A1*. While differentiated cells are most susceptible to wCS exposure, the exposure of submerged basal cells to CSE provides a technologically simpler, fast and efficient exposure setting to assess CS-regulated genes and may be particularly suited to assess regulation by CS under conditions of bronchial epithelial injury. CSE exposure of bronchial epithelial cells during the full period of differentiation on the other hand may be the model of choice when chronic CS exposure needs to be assessed. Overall, our findings provide important guidelines for the design of human cigarette smoke-induced *in vitro* models, in particular when using CSE instead of wCS.

SUPPLEMENTAL DATA

Supplemental Tables S1-S4, and Supplemental Figures S1–S9 are available at: https://doi.org/10.6084/m9.figshare.16713784.

ACKNOWLEDGEMENTS

We gratefully acknowledge the provision of human biomaterial and clinical data from the CPC-M bioArchive and its partners at the Asklepios Biobank Gauting, the Klinikum der Universität München and the Ludwig-Maximilians-Universität München. This work was supported by the Deutsche Forschungsgemeinschaft (DFG) within the Research Training Group GRK2338 (MM, grant to CASW), the Helmholtz Association, the German Center for Lung Research (DZL), and the Federal Institute for Risk Assessment (Bundesinstitut für Risikobewertung, BfR) within the Bf3R Research Funding Program in the area of 3R - Replacement, Reduction and Refinement (#1328-570, AC, grant to CASW). We gratefully acknowledge Mircea-Gabriel Stoleriu, Misako Nakayama and Annika Frank for providing their expertise and helpful discussions during this study, Hannah Marchi for statistical consulting, and Ceylan Onursal for help with artwork.

Downloaded from journals.physiology.org/journal/ajplung at Helmholtz Zentrum Muenchen (146.107.008.161) on December 16, 2021.

REFERENCES

1. **Chang SA**. Smoking and type 2 diabetes mellitus. *Diabetes Metab J* 36: 399-403, 2012.
2. **Durazzo TC, Mattsson N, Weiner MW, and Alzheimer's Disease Neuroimaging I**. Smoking and increased Alzheimer's disease risk: a review of potential mechanisms. *Alzheimers Dement* 10: S122-145, 2014.
3. **Jha P, MacLennan M, Chaloupka FJ, Yurekli A, Ramasundarahettige C, Palipudi K, Zatonksi W, Asma S, and Gupta PC**. Global Hazards of Tobacco and the Benefits of Smoking Cessation and Tobacco Taxes. In: *Cancer: Disease Control Priorities, Third Edition (Volume 3)*, edited by Gelband H, Jha P, Sankaranarayanan R, and Horton S. Washington (DC): 2015.
4. The top 10 causes of death. World Health Organisation. https://www.who.int/news-room/fact-sheets/detail/the-top-10-causes-of-death. [20 Oct, 2020].
5. **Tam A, Wadsworth S, Dorscheid D, Man SF, and Sin DD**. The airway epithelium: more than just a structural barrier. *Ther Adv Respir Dis* 5: 255-273, 2011.
6. **Hiemstra PS, McCray PB, Jr., and Bals R**. The innate immune function of airway epithelial cells in inflammatory lung disease. *The European respiratory journal* 45: 1150-1162, 2015.
7. **Montoro DT, Haber AL, Biton M, Vinarsky V, Lin B, Birket SE, Yuan F, Chen S, Leung HM, Villoria J, Rogel N, Burgin G, Tsankov AM, Waghray A, Slyper M, Waldman J, Nguyen L, Dionne D, Rozenblatt-Rosen O, Tata PR, Mou H, Shivaraju M, Bihler H, Mense M, Tearney GJ, Rowe SM, Engelhardt JF, Regev A, and Rajagopal J**. A revised airway epithelial hierarchy includes CFTR-expressing ionocytes. *Nature* 560: 319-324, 2018.
8. **Davis JD, and Wypych TP**. Cellular and functional heterogeneity of the airway epithelium. *Mucosal Immunol* 2021.
9. **Schamberger AC, Staab-Weijnitz CA, Mise-Racek N, and Eickelberg O**. Cigarette smoke alters primary human bronchial epithelial cell differentiation at the air-liquid interface. *Sci Rep* 5: 8163, 2015.
10. **Heijink IH, Brandenburg SM, Postma DS, and van Oosterhout AJ**. Cigarette smoke impairs airway epithelial barrier function and cell-cell contact recovery. *Eur Respir J* 39: 419-428, 2012.
11. **Zhang S, Li X, Xie F, Liu K, Liu H, and Xie J**. Evaluation of whole cigarette smoke induced oxidative stress in A549 and BEAS-2B cells. *Environ Toxicol Pharmacol* 54: 40-47, 2017.
12. **Pouwels SD, Zijlstra GJ, van der Toorn M, Hesse L, Gras R, Ten Hacken NH, Krysko DV, Vandenabeele P, de Vries M, van Oosterhout AJ, Heijink IH, and Nawijn MC**. Cigarette smoke-induced necroptosis and DAMP release trigger neutrophilic airway inflammation in mice. *Am J Physiol Lung Cell Mol Physiol* 310: L377-386, 2016.
13. **Long C, Lai Y, Li T, Nyunoya T, and Zou C**. Cigarette smoke extract modulates Pseudomonas aeruginosa bacterial load via USP25/HDAC11 axis in lung epithelial cells. *Am J Physiol Lung Cell Mol Physiol* 318: L252-L263, 2020.
14. **Phillips J, Kluss B, Richter A, and Massey E**. Exposure of bronchial epithelial cells to whole cigarette smoke: assessment of cellular responses. *Altern Lab Anim* 33: 239-248, 2005.
15. **Nishida K, Brune KA, Putcha N, Mandke P, O'Neal WK, Shade D, Srivastava V, Wang M, Lam H, An SS, Drummond MB, Hansel NN, Robinson DN, and Sidhaye VK**. Cigarette smoke disrupts monolayer integrity by altering epithelial cell-cell adhesion and cortical tension. *Am J Physiol Lung Cell Mol Physiol* 313: L581-L591, 2017.
16. **Wu YP, Cao C, Wu YF, Li M, Lai TW, Zhu C, Wang Y, Ying SM, Chen ZH, Shen HH, and Li W**. Activating transcription factor 3 represses cigarette smoke-induced IL6 and IL8 expression via suppressing NF-kappaB activation. *Toxicol Lett* 270: 17-24, 2017.
17. **Thaikoottathil JV, Martin RJ, Zdunek J, Weinberger A, Rino JG, and Chu HW**. Cigarette smoke extract reduces VEGF in primary human airway epithelial cells. *Eur Respir J* 33: 835-843, 2009.
18. **Jukosky J, Gosselin BJ, Foley L, Dechen T, Fiering S, and Crane-Godreau MA**. In vivo Cigarette Smoke Exposure Decreases CCL20, SLPI, and BD-1 Secretion by Human Primary Nasal Epithelial Cells. *Front Psychiatry* 6: 185, 2015.

Downloaded from journals.physiology.org/journal/ajplung at Helmholtz Zentrum Muenchen (146.107.008.161) on December 16, 2021.

19. **Yanagisawa S, Baker JR, Vuppusetty C, Koga T, Colley T, Fenwick P, Donnelly LE, Barnes PJ, and Ito K**. The dynamic shuttling of SIRT1 between cytoplasm and nuclei in bronchial epithelial cells by single and repeated cigarette smoke exposure. *PLoS One* 13: e0193921, 2018.
20. **Wong FH, AbuArish A, Matthes E, Turner MJ, Greene LE, Cloutier A, Robert R, Thomas DY, Cosa G, Cantin AM, and Hanrahan JW**. Cigarette smoke activates CFTR through ROS-stimulated cAMP signaling in human bronchial epithelial cells. *Am J Physiol Cell Physiol* 314: C118-C134, 2018.
21. **Andrault PM, Schamberger AC, Chazeirat T, Sizaret D, Renault J, Staab-Weijnitz CA, Hennen E, Petit-Courty A, Wartenberg M, Saidi A, Baranek T, Guyetant S, Courty Y, Eickelberg O, Lalmanach G, and Lecaille F**. Cigarette smoke induces overexpression of active human cathepsin S in lungs from current smokers with or without COPD. 317: L625-L638, 2019.
22. **Starke RM, Ali MS, Jabbour PM, Tjoumakaris SI, Gonzalez F, Hasan DM, Rosenwasser RH, Owens GK, Koch WJ, and Dumont AS**. Cigarette smoke modulates vascular smooth muscle phenotype: implications for carotid and cerebrovascular disease. *PLoS One* 8: e71954, 2013.
23. **van der Toorn M, Sewer A, Marescotti D, Johne S, Baumer K, Bornand D, Dulize R, Merg C, Corciulo M, Scotti E, Pak C, Leroy P, Guedj E, Ivanov N, Martin F, Peitsch M, Hoeng J, and Luettich K**. The biological effects of long-term exposure of human bronchial epithelial cells to total particulate matter from a candidate modified-risk tobacco product. *Toxicol In Vitro* 50: 95-108, 2018.
24. **Mathis C, Poussin C, Weisensee D, Gebel S, Hengstermann A, Sewer A, Belcastro V, Xiang Y, Ansari S, Wagner S, Hoeng J, and Peitsch MC**. Human bronchial epithelial cells exposed in vitro to cigarette smoke at the air-liquid interface resemble bronchial epithelium from human smokers. *American Journal of Physiology-Lung Cellular and Molecular Physiology* 304: L489-L503, 2013.
25. **Gindele JA, Kiechle T, Benediktus K, Birk G, Brendel M, Heinemann F, Wohnhaas CT, LeBlanc M, Zhang H, Strulovici-Barel Y, Crystal RG, Thomas MJ, Stierstorfer B, Quast K, and Schymeinsky J**. Intermittent exposure to whole cigarette smoke alters the differentiation of primary small airway epithelial cells in the air-liquid interface culture. *Sci Rep* 10: 6257, 2020.
26. **Gelbman BD, Heguy A, O'Connor TP, Zabner J, and Crystal RG**. Upregulation of pirin expression by chronic cigarette smoking is associated with bronchial epithelial cell apoptosis. *Respiratory Research* 8: 10, 2007.
27. **Wang R, Wang G, Ricard MJ, Ferris B, Strulovici-Barel Y, Salit J, Hackett NR, Gudas LJ, and Crystal RG**. Smoking-induced upregulation of AKR1B10 expression in the airway epithelium of healthy individuals. *Chest* 138: 1402-1410, 2010.
28. **Gower AC, Steiling K, Brothers JF, 2nd, Lenburg ME, and Spira A**. Transcriptomic studies of the airway field of injury associated with smoking-related lung disease. *Proc Am Thorac Soc* 8: 173-179, 2011.
29. **Van Dyck E, Nazarov PV, Muller A, Nicot N, Bosseler M, Pierson S, Van Moer K, Palissot V, Mascaux C, Knolle U, Ninane V, Nati R, Bremnes RM, Vallar L, Berchem G, and Schlesser M**. Bronchial airway gene expression in smokers with lung or head and neck cancer. *Cancer Medicine* 3: 322-336, 2014.
30. **Yang CX, Shi H, Ding I, Milne S, Hernandez Cordero AI, Yang CWT, Kim EK, Hackett TL, Leung J, Sin DD, and Obeidat M**. Widespread Sexual Dimorphism in the Transcriptome of Human Airway Epithelium in Response to Smoking. *Sci Rep* 9: 17600, 2019.
31. **Duclos GE, Teixeira VH, Autissier P, Gesthalter YB, Reinders-Luinge MA, Terrano R, Dumas YM, Liu G, Mazzilli SA, Brandsma CA, van den Berge M, Janes SM, Timens W, Lenburg ME, Spira A, Campbell JD, and Beane J**. Characterizing smoking-induced transcriptional heterogeneity in the human bronchial epithelium at single-cell resolution. *Sci Adv* 5: eaaw3413, 2019.
32. **Spira A, Beane J, Shah V, Liu G, Schembri F, Yang X, Palma J, and Brody JS**. Effects of cigarette smoke on the human airway epithelial cell transcriptome. *Proc Natl Acad Sci U S A* 101: 10143-10148, 2004.
33. **Harvey BG, Heguy A, Leopold PL, Carolan BJ, Ferris B, and Crystal RG**. Modification of gene expression of the small airway epithelium in response to cigarette smoking. *J Mol Med (Berl)* 85: 39-53, 2007.
34. **Beane J, Sebastiani P, Liu G, Brody JS, Lenburg ME, and Spira A**. Reversible and permanent effects of tobacco smoke exposure on airway epithelial gene expression. *Genome Biol* 8: R201, 2007.

Downloaded from journals.physiology.org/journal/ajplung at Helmholtz Zentrum Muenchen (146.107.008.161) on December 16, 2021.

35. **Shaykhiev R, Otaki F, Bonsu P, Dang DT, Teater M, Strulovici-Barel Y, Salit J, Harvey BG, and Crystal RG**. Cigarette smoking reprograms apical junctional complex molecular architecture in the human airway epithelium in vivo. *Cell Mol Life Sci* 68: 877-892, 2011.
36. **Walters MS, De BP, Salit J, Buro-Auriemma LJ, Wilson T, Rogalski AM, Lief L, Hackett NR, Staudt MR, Tilley AE, Harvey B-G, Kaner RJ, Mezey JG, Ashbridge B, Moore MAS, and Crystal RG**. Smoking accelerates aging of the small airway epithelium. *Respiratory Research* 15: 94, 2014.
37. **Murray LA, Dunmore R, Camelo A, Da Silva CA, Gustavsson MJ, Habiel DM, Hackett TL, Hogaboam CM, Sleeman MA, and Knight DA**. Acute cigarette smoke exposure activates apoptotic and inflammatory programs but a second stimulus is required to induce epithelial to mesenchymal transition in COPD epithelium. *Respir Res* 18: 82, 2017.
38. **Voic H, Li X, Jang J-H, Zou C, Sundd P, Alder J, Rojas M, Chandra D, Randell S, Mallampalli RK, Tesfaigzi Y, Ryba T, and Nyunoya T**. RNA sequencing identifies common pathways between cigarette smoke exposure and replicative senescence in human airway epithelia. *BMC Genomics* 20: 22, 2019.
39. **Comer DM, Elborn JS, and Ennis M**. Comparison of nasal and bronchial epithelial cells obtained from patients with COPD. *PLoS One* 7: e32924, 2012.
40. **Higham A, Bostock D, Booth G, Dungwa JV, and Singh D**. The effect of electronic cigarette and tobacco smoke exposure on COPD bronchial epithelial cell inflammatory responses. *Int J Chron Obstruct Pulmon Dis* 13: 989-1000, 2018.
41. **Bucchieri F, Marino Gammazza A, Pitruzzella A, Fucarino A, Farina F, Howarth P, Holgate ST, Zummo G, and Davies DE**. Cigarette smoke causes caspase-independent apoptosis of bronchial epithelial cells from asthmatic donors. *PLoS One* 10: e0120510, 2015.
42. **Liang Y, Tian L, Ho K-F, Ip MS-M, and Mak JC-W**. Comparisons on mitochondrial function following exposure of cigarette smoke extract and fine particulate matter in human bronchial epithelial cells. *Eur Respir J* 54: PA2436, 2019.
43. **Ito S, Ishimori K, and Ishikawa S**. Effects of repeated cigarette smoke extract exposure over one month on human bronchial epithelial organotypic culture. *Toxicol Rep* 5: 864-870, 2018.
44. **Schamberger AC, Mise N, Jia J, Genoyer E, Yildirim AO, Meiners S, and Eickelberg O**. Cigarette smoke-induced disruption of bronchial epithelial tight junctions is prevented by transforming growth factor-beta. *Am J Respir Cell Mol Biol* 50: 1040-1052, 2014.
45. **Bitterle E, Karg E, Schroeppel A, Kreyling WG, Tippe A, Ferron GA, Schmid O, Heyder J, Maier KL, and Hofer T**. Dose-controlled exposure of A549 epithelial cells at the air-liquid interface to airborne ultrafine carbonaceous particles. *Chemosphere* 65: 1784-1790, 2006.
46. **Lenz AG, Karg E, Brendel E, Hinze-Heyn H, Maier KL, Eickelberg O, Stoeger T, and Schmid O**. Inflammatory and oxidative stress responses of an alveolar epithelial cell line to airborne zinc oxide nanoparticles at the air-liquid interface: a comparison with conventional, submerged cell-culture conditions. *Biomed Res Int* 2013: 652632, 2013.
47. **Serediouk V**. Wirkung von Zigarettenrauch auf Lungenzellen in vitro: Etablierung eines Zigarettenrauch-Zell-Expositionssystems (Unpublished Master's thesis). In: *Fakultät Biotechnologie und Bioinformatik* Hochschule Weihenstephan-Triesdorf, 2016.
48. **Boers JE, Ambergen AW, and Thunnissen FB**. Number and proliferation of basal and parabasal cells in normal human airway epithelium. *Am J Respir Crit Care Med* 157: 2000-2006, 1998.
49. **Boers JE, Ambergen AW, and Thunnissen FB**. Number and proliferation of clara cells in normal human airway epithelium. *Am J Respir Crit Care Med* 159: 1585-1591, 1999.
50. **Rogers DF**. The airway goblet cell. *The International Journal of Biochemistry & Cell Biology* 35: 1-6, 2003.
51. **Srinivasan B, Kolli AR, Esch MB, Abaci HE, Shuler ML, and Hickman JJ**. TEER measurement techniques for in vitro barrier model systems. *J Lab Autom* 20: 107-126, 2015.
52. **Chen M, Yang T, Meng X, and Sun T**. Azithromycin attenuates cigarette smoke extract-induced oxidative stress injury in human alveolar epithelial cells. *Mol Med Rep* 11: 3414-3422, 2015.
53. **Ferraro M, Gjomarkaj M, Siena L, Di Vincenzo S, and Pace E**. Formoterol and fluticasone propionate combination improves histone deacetylation and anti-inflammatory activities in bronchial

Downloaded from journals.physiology.org/journal/ajplung at Helmholtz Zentrum Muenchen (146.107.008.161) on December 16, 2021.

epithelial cells exposed to cigarette smoke. *Biochim Biophys Acta Mol Basis Dis* 1863: 1718-1727, 2017.

54. **Qin H, Gao F, Wang Y, Huang B, Peng L, Mo B, and Wang C**. Nur77 promotes cigarette smokeinduced autophagic cell death by increasing the dissociation of Bcl2 from Beclin-1. *Int J Mol Med* 44: 25-36, 2019.

55. **Amatngalim GD, van Wijck Y, de Mooij-Eijk Y, Verhoosel RM, Harder J, Lekkerkerker AN, Janssen RA, and Hiemstra PS**. Basal cells contribute to innate immunity of the airway epithelium through production of the antimicrobial protein RNase 7. *J Immunol* 194: 3340-3350, 2015.

56. **Benam KH, Novak R, Nawroth J, Hirano-Kobayashi M, Ferrante TC, Choe Y, Prantil-Baun R, Weaver JC, Bahinski A, Parker KK, and Ingber DE**. Matched-Comparative Modeling of Normal and Diseased Human Airway Responses Using a Microengineered Breathing Lung Chip. *Cell Syst* 3: 456-466 e454, 2016.

57. **Thorne D, Kilford J, Payne R, Adamson J, Scott K, Dalrymple A, Meredith C, and Dillon D**. Characterisation of a Vitrocell(R) VC 10 in vitro smoke exposure system using dose tools and biological analysis. *Chem Cent J* 7: 146, 2013.

58. **Robinson RJ, and Yu CP**. Deposition of cigarette smoke particles in the human respiratory tract. *Aerosol Sci Technol* 34: 202-215, 2001.

59. **Paur HR, Cassee FR, Teeguarden J, Fissan H, Diabate S, Aufderheide M, Kreyling WG, Hanninen O, Kasper G, Riediker M, Rothen-Rutishauser B, and Schmid O**. In-vitro cell exposure studies for the assessment of nanoparticle toxicity in the lung-A dialog between aerosol science and biology. *J Aerosol Sci* 42: 668-692, 2011.

60. **Parrish ME, Lyons-Hart JL, and Shafer KH**. Puff-by-puff and intrapuff analysis of cigarette smoke using infrared spectroscopy. *Vib Spectrosc* 27: 29-42, 2001.

61. **Balashazy I, Hofmann W, and Heistracher T**. Local particle deposition patterns may play a key role in the development of lung cancer. *J Appl Physiol (1985)* 94: 1719-1725, 2003.

62. **Heyder J**. Deposition of inhaled particles in the human respiratory tract and consequences for regional targeting in respiratory drug delivery. *Proc Am Thorac Soc* 1: 315-320, 2004.

63. **Brody JS**. Transcriptome alterations induced by cigarette smoke. *Int J Cancer* 131: 2754-2762, 2012.

64. **Balásházy I, Hofmann W, and Heistracher T**. Computation of local enhancement factors for the quantification of particle deposition patterns in airway bifurcations. *J Aerosol Sci* 30: 185-203, 1999.

65. **Mossina A, Lukas C, Merl-Pham J, Uhl FE, Mutze K, Schamberger A, Staab-Weijnitz C, Jia J, Yildirim AO, Konigshoff M, Hauck SM, Eickelberg O, and Meiners S**. Cigarette smoke alters the secretome of lung epithelial cells. *Proteomics* 17: 2017.

66. **Tatsuta M, Kan OK, Ishii Y, Yamamoto N, Ogawa T, Fukuyama S, Ogawa A, Fujita A, Nakanishi Y, and Matsumoto K**. Effects of cigarette smoke on barrier function and tight junction proteins in the bronchial epithelium: protective role of cathelicidin LL-37. *Respir Res* 20: 251, 2019.

67. **Faiz A, Heijink IH, Vermeulen CJ, Guryev V, van den Berge M, Nawijn MC, and Pouwels SD**. Cigarette smoke exposure decreases CFLAR expression in the bronchial epithelium, augmenting susceptibility for lung epithelial cell death and DAMP release. *Sci Rep* 8: 12426, 2018.

68. **Simet SM, Sisson JH, Pavlik JA, Devasure JM, Boyer C, Liu X, Kawasaki S, Sharp JG, Rennard SI, and Wyatt TA**. Long-term cigarette smoke exposure in a mouse model of ciliated epithelial cell function. *Am J Respir Cell Mol Biol* 43: 635-640, 2010.

69. **Pickett G, Seagrave J, Boggs S, Polzin G, Richter P, and Tesfaigzi Y**. Effects of 10 cigarette smoke condensates on primary human airway epithelial cells by comparative gene and cytokine expression studies. *Toxicol Sci* 114: 79-89, 2010.

70. **Zevin S, and Benowitz NL**. Drug Interactions with Tobacco Smoking. *Clin Pharmacokinet* 36: 425-438, 1999.

71. **Guerrina N, Traboulsi H, Eidelman DH, and Baglole CJ**. The Aryl Hydrocarbon Receptor and the Maintenance of Lung Health. *Int J Mol Sci* 19: 2018.

Downloaded from journals.physiology.org/journal/ajplung at Helmholtz Zentrum Muenchen (146.107.008.161) on December 16, 2021.

72. **Nebert DW, Roe AL, Dieter MZ, Solis WA, Yang Y, and Dalton TP**. Role of the aromatic hydrocarbon receptor and [Ah] gene battery in the oxidative stress response, cell cycle control, and apoptosis. *Biochem Pharmacol* 59: 65-85, 2000.
73. **Murray GI, Melvin WT, Greenlee WF, and Burke MD**. Regulation, Function, and Tissue-Specific Expression of Cytochrome P450 CYP1B1. *Annu Rev Pharmacool Toxicol* 41: 297-316, 2001.
74. **Miao W, Hu L, Scrivens PJ, and Batist G**. Transcriptional regulation of NF-E2 p45-related factor (NRF2) expression by the aryl hydrocarbon receptor-xenobiotic response element signaling pathway: direct cross-talk between phase I and II drug-metabolizing enzymes. *J Biol Chem* 280: 20340-20348, 2005.
75. **Rangasamy T, Cho CY, Thimmulappa RK, Zhen L, Srisuma SS, Kensler TW, Yamamoto M, Petrache I, Tuder RM, and Biswal S**. Genetic ablation of Nrf2 enhances susceptibility to cigarette smoke–induced emphysema in mice. *The Journal of Clinical Investigation* 114: 1248-1259, 2004.
76. **Cho HY, Reddy SP, Debiase A, Yamamoto M, and Kleeberger SR**. Gene expression profiling of NRF2-mediated protection against oxidative injury. *Free Radic Biol Med* 38: 325-343, 2005.
77. **Penning TM**. Aldo-Keto Reductase Regulation by the Nrf2 System: Implications for Stress Response, Chemotherapy Drug Resistance, and Carcinogenesis. *Chem Res Toxicol* 30: 162-176, 2017.
78. **Nishinaka T, Miura T, Okumura M, Nakao F, Nakamura H, and Terada T**. Regulation of aldo–keto reductase AKR1B10 gene expression: Involvement of transcription factor Nrf2. *Chem Biol Interact* 191: 185-191, 2011.
79. **Lou H, Du S, Ji Q, and Stolz A**. Induction of AKR1C2 by Phase II Inducers: Identification of a Distal Consensus Antioxidant Response Element Regulated by NRF2. *Mol Pharmacol* 69: 1662-1672, 2006.
80. **Thimmulappa RK, Mai KH, Srisuma S, Kensler TW, Yamamoto M, and Biswal S**. Identification of Nrf2-regulated genes induced by the chemopreventive agent sulforaphane by oligonucleotide microarray. *Cancer Res* 62: 5196-5203, 2002.
81. **Chan K, and Kan YW**. Nrf2 is essential for protection against acute pulmonary injury in mice. *Proc Natl Acad Sci U S A* 96: 12731-12736, 1999.
82. **Brzóska K, Stępkowski TM, and Kruszewski M**. Basal PIR expression in HeLa cells is driven by NRF2 via evolutionary conserved antioxidant response element. *Mol Cell Biochem* 389: 99-111, 2014.
83. **Namani A, Matiur Rahaman M, Chen M, and Tang X**. Gene-expression signature regulated by the KEAP1-NRF2-CUL3 axis is associated with a poor prognosis in head and neck squamous cell cancer. *BMC Cancer* 18: 46, 2018.
84. **Morel Y, Mermod N, and Barouki R**. An autoregulatory loop controlling CYP1A1 gene expression: role of H(2)O(2) and NFI. *Mol Cell Biol* 19: 6825-6832, 1999.
85. **Dietrich C**. Antioxidant Functions of the Aryl Hydrocarbon Receptor. *Stem Cells International* 2016: 7943495, 2016.
86. **Di YP, Zhao J, and Harper R**. Cigarette smoke induces MUC5AC protein expression through the activation of Sp1. *J Biol Chem* 287: 27948-27958, 2012.
87. **Di Sano C, D'Anna C, Ferraro M, Chiappara G, and Pace E**. Notch-1 expression is increased by cigarette smoke exposure and its activation up-regulates ki67, PCNA proliferative markers and actin polymerizations in bronchial epithelial cells. *Eur Respir J* 54: PA2399, 2019.
88. **Ou-Yang HF, Wu CG, Qu SY, and Li ZK**. Notch signaling downregulates MUC5AC expression in airway epithelial cells through Hes1-dependent mechanisms. *Respiration* 86: 341-346, 2013.
89. **Yin SJ, Chou CF, Lai CL, Lee SL, and Han CL**. Human class IV alcohol dehydrogenase: kinetic mechanism, functional roles and medical relevance. *Chem Biol Interact* 143-144: 219-227, 2003.
90. **Jelski W, Chrostek L, Szmitkowski M, and Laszewicz W**. Activity of class I, II, III, and IV alcohol dehydrogenase isoenzymes in human gastric mucosa. *Dig Dis Sci* 47: 1554-1557, 2002.
91. **Duester G, Shean ML, McBride MS, and Stewart MJ**. Retinoic acid response element in the human alcohol dehydrogenase gene ADH3: implications for regulation of retinoic acid synthesis. *Mol Cell Biol* 11: 1638-1646, 1991.
92. **Balmer JE, and Blomhoff R**. Gene expression regulation by retinoic acid. *J Lipid Res* 43: 1773-1808, 2002.

Downloaded from journals.physiology.org/journal/ajplung at Helmholtz Zentrum Muenchen (146.107.008.161) on December 16, 2021.

93. **Fulcher ML, Gabriel S, Burns KA, Yankaskas JR, and Randell SH**. Well-Differentiated Human Airway Epithelial Cell Cultures. In: *Human Cell Culture Protocols*, edited by Picot J. Totowa, NJ: Humana Press, 2005, p. 183-206.

94. **Rayner RE, Makena P, Prasad GL, and Cormet-Boyaka E**. Optimization of Normal Human Bronchial Epithelial (NHBE) Cell 3D Cultures for in vitro Lung Model Studies. *Sci Rep* 9: 500, 2019.

95. **Leung JM, Yang CX, Tam A, Shaipanich T, Hackett T-L, Singhera GK, Dorscheid DR, and Sin DD**. ACE-2 Expression in the Small Airway Epithelia of Smokers and COPD Patients: Implications for COVID-19. *Eur Respir J* 2000688, 2020.

96. **Ross D, and Siegel D**. NAD(P)H:quinone oxidoreductase 1 (NQO1, DT-diaphorase), functions and pharmacogenetics. *Methods Enzymol* 382: 115-144, 2004.

97. **Siegel D, Franklin WA, and Ross D**. Immunohistochemical detection of NAD(P)H:quinone oxidoreductase in human lung and lung tumors. *Clin Cancer Res* 4: 2065-2070, 1998.

98. **Carolan BJ, Heguy A, Harvey BG, Leopold PL, Ferris B, and Crystal RG**. Up-regulation of expression of the ubiquitin carboxyl-terminal hydrolase L1 gene in human airway epithelium of cigarette smokers. *Cancer Res* 66: 10729-10740, 2006.

99. **Osaka H, Wang YL, Takada K, Takizawa S, Setsuie R, Li H, Sato Y, Nishikawa K, Sun YJ, Sakurai M, Harada T, Hara Y, Kimura I, Chiba S, Namikawa K, Kiyama H, Noda M, Aoki S, and Wada K**. Ubiquitin carboxy-terminal hydrolase L1 binds to and stabilizes monoubiquitin in neuron. *Hum Mol Genet* 12: 1945-1958, 2003.

100. **Brinkmann K, Zigrino P, Witt A, Schell M, Ackermann L, Broxtermann P, Schull S, Andree M, Coutelle O, Yazdanpanah B, Seeger JM, Klubertz D, Drebber U, Hacker UT, Kronke M, Mauch C, Hoppe T, and Kashkar H**. Ubiquitin C-terminal hydrolase-L1 potentiates cancer chemosensitivity by stabilizing NOXA. *Cell Rep* 3: 881-891, 2013.

101. **Teeguarden JG, Hinderliter PM, Orr G, Thrall BD, and Pounds JG**. Particokinetics in vitro: dosimetry considerations for in vitro nanoparticle toxicity assessments. *Toxicol Sci* 95: 300-312, 2007.

102. **Schumacher JN, Green CR, Best FW, and Newell MP**. Smoke composition. An extensive investigation of the water-soluble portion of cigarette smoke. *J Agric Food Chem* 25: 310-320, 1977.

103. **Larigot L, Juricek L, Dairou J, and Coumoul X**. AhR signaling pathways and regulatory functions. *Biochim Open* 7: 1-9, 2018.

104. **Bourgeois JS, Jacob J, Garewal A, Ndahayo R, and Paxson J**. The Bioavailability of Soluble Cigarette Smoke Extract Is Reduced through Interactions with Cells and Affects the Cellular Response to CSE Exposure. *PLOS ONE* 11: e0163182, 2016.

Downloaded from journals.physiology.org/journal/ajplung at Helmholtz Zentrum Muenchen (146.107.008.161) on December 16, 2021.

FIGURE LEGENDS

Figure 1. Differentiation of primary bronchial epithelial cells at the air-liquid-interface. (A) Schematic overview of expansion and differentiation of bronchial epithelial cells. During the expansion phase, basal cells were cultured on regular tissue culture plastic, followed by seeding on transwells. Upon reaching confluency, the apical medium was removed to create an air-liquid interface, which was maintained throughout differentiation into a pseudostratified epithelium for 28 days. **(B)** Representative immunofluorescent stainings for cell-type specific markers including tumor protein 63 (p63), acetylated tubulin (acTub), Club cells 10 kDa secretory protein (CC10), and mucin 5AC (MUC5AC) for basal, ciliated, club, and goblet cells, respectively, confirmed differentiation into a full-blown bronchial epithelium over time. Results shown are representative for n=4. **(C)** Quantification of all main bronchial epithelial cell types from immunofluorescent stainings demonstrate increase of ciliated, club, and goblet cells at the expense of basal cells. Results shown are derived from n=4 (independent donors) and given as mean ± SD. **(D)** Epithelial barrier integrity, as assessed by transepithelial electrical resistance (TEER), stabilized over the course of differentiation. Results shown are derived from n=5 (independent donors) and given as mean ± SD. Scale bar, 40µm.

Figure 2. Exposure of basal primary human bronchial epithelial cells under submerged conditions to cigarette smoke extract (CSE) resulted in upregulation of six out of nine smoke exposure regulated genes (SERGs). (**A**) Experimental set-up. Non-differentiated phBECs were exposed to 0, 2.5, 5.0, 10 and 20% CSE under submerged conditions for 24 h, followed by collection of RNA and protein. (**B**) Results of RT-qPCR are presented as fold change of 9 genes relative to control normalized to 1 (red line). Mucin 5AC (MUC5AC) was not expressed under these conditions and thus not included. Genes are shown in order of regulation strength in current smokers from highest (left) to lowest (right) fold change (see Table 1). Hydroxymethylbilane synthase transcript (HMBS) was used as internal reference gene. Statistical analysis was assessed by repeated measures ANOVA with Bonferroni correction for multiple comparisons (*, $p<0.05$; **, $p<0.01$; ***, $p<0.001$). (**C**) Representative Western Blots for four selected SERGs show dose-dependent regulation also on protein level. β-actin (ACTB) was used as loading control. Results shown are based on n= 4 (independent donors) and given as mean ± SD.

Figure 3. Chronic basolateral exposure of primary human bronchial epithelial cells during the complete course of differentiation resulted in significant upregulation of seven out of 10 smoke exposure regulated genes (SERGs). (A) Experimental set-up. PhBECs were chronically exposed to 5% CSE in the basolateral compartment from day 0 to day 28 of differentiation. **(B)** Results of RT-qPCR are presented as fold change relative to control normalized to 1 (red line). Genes are shown in order of regulation strength in current smokers from highest (left) to lowest (right) fold change (see Table

Downloaded from journals.physiology.org/journal/ajplung at Helmholtz Zentrum Muenchen (146.107.008.161) on December 16, 2021.

1). WD repeat-containing protein 89 (WDR89) transcript was used as internal reference gene. Statistical analysis was assessed by repeated measures ANOVA followed by Bonferroni correction for multiple comparisons (p<0.05; *, p<0.05; **, p<0.01; ***, p<0.001). **(C)** In agreement with transcript data, representative Western Blots for four selected SERGs show regulation on protein level for ALDH3A1 and NQO1, but less prominently for AKR1B10 and AKR1C1. β-actin (ACTB) was used as loading control. Results shown are based on n= 5 (independent donors) and given as mean ± SD.

Figure 4. Short acute apical exposure of differentiated primary human bronchial epithelial cells with whole cigarette smoke (wCS) and cigarette smoke extract (CSE) using comparable CS particulate doses resulted in significant upregulation of six out of 10 smoke exposure regulated genes (SERGs) for wCS, but none for CSE. (A) Experimental set-up. Fully differentiated phBECs were either exposed apically to 200 µl of 40% CSE for 5 min or to 5 min exposure to wCS generated by 3 cm of a research grade cigarette followed by culture of cells for 24 h and sample collection for mRNA and protein analysis. **(B)** Results of RT-qPCR are presented as fold change of 10 genes relative to control normalized to 1 (red line). WD repeat-containing protein 89 (WDR89) transcript was used as internal reference gene. Statistical analyses was performed using two tailed student's *t*-test (*, p<0.05; **, p<0,01; ***, p<0.001). **(C)** Representative Western Blots for 4 selected SERGs show no upregulation on protein level for CSE, but moderate upregulation for all 4 for wCS. β-actin (ACTB) was used as loading control. **(D)** Representative immunofluorescent stainings demonstrate increases in the number of AKR1C1^{+}, NQO1^{+}, PIR^{+}. and UCHL1^{+} cells. Scale bar 40 µm. Results shown are based on n= 5 (independent donors) and given as mean ± SD.

Figure 5. Acute apical exposure of differentiated primary human epithelial cells with cigarette smoke extract (CSE) resulted in significant upregulation of one out of 10 smoke exposure regulated gene (SERGs). (A) Experimental set-up. Fully differentiated phBECs were exposed apically to 200 µl of 0% 3%, 6%, 12% CSE for 24 h followed by collection of cells for mRNA and protein analysis. **(B)** Results of RT-qPCR are presented as fold change of 10 genes relative to control normalized to 1 (red line). Genes are shown in order of regulation strength in current smokers from highest (left) to lowest (right) fold change (see Table 1). Hypoxanthine-guanine phosphoribosyltransferase (HPRT) was used as internal reference gene. Statistical analysis was assessed by repeated measures ANOVA with Bonferroni correction for multiple comparisons (*, p<0.05). **(C)** Representative Western Blots for four selected SERGs show no regulation on protein level. β-actin (ACTB) was used as loading control. Results shown are based on n= 4 (independent donors) and given as mean ± SD.

Figure 6. Acute basolateral exposure of fully differentiated primary human bronchial epithelial cells resulted in significant upregulation of one out of 10 smoke exposure regulated genes (SERGs). (A) Experimental setup. Fully differentiated phBECs were exposed basolaterally to 5 % cigarette smoke

Downloaded from journals.physiology.org/journal/ajplung at Helmholtz Zentrum Muenchen (146.107.008.161) on December 16, 2021.

extract (CSE) for 24 h followed by collection of cells for mRNA and protein analysis. **(B)** Results of RT-qPCR (n=5) are presented as fold change of 10 genes relative to control normalized to 1 (dotted line). Genes are shown in order of regulation strength in current smokers from highest (left) to lowest (right) fold change (see Table 1). Polyubiquitin-C (UBC) was used as a housekeeper gene. Statistical analyses were performed using paired two tailed *t*-test ($p<0.05$). **(C)** Western Blots (n=5) are shown for 4 assessed genes. β-actin (ACTB) was used as loading control. Results shown are based on n= 5 (independent donors) and given as mean ± SD.

Figure 7. Immunofluorescent stainings for assessment of cell-type-specific expression of selected smoke exposure regulated genes (SERGs). Representative immunofluorescent stainings (n=3) of primary human bronchial epithelial cells (phBECs) exposed to whole cigarette smoke (wCS) demonstrate expression of all selected SERGs in basal cells ($p63^+$ cells). In addition, NQO1, PIR, and UCHL1 are expressed by ciliated cells ($acTub^+$ cells), and AKR1C1 by club cells ($CC10^+$ cells). Scale bars, 50µm and 20µm. For more co-stainings with cell-type-specific markers, the reader is referred to supplementary figure S6. Results shown are based on n= 3 (independent donors).

Downloaded from journals.physiology.org/journal/ajplung at Helmholtz Zentrum Muenchen (146.107.008.161) on December 16, 2021.

A

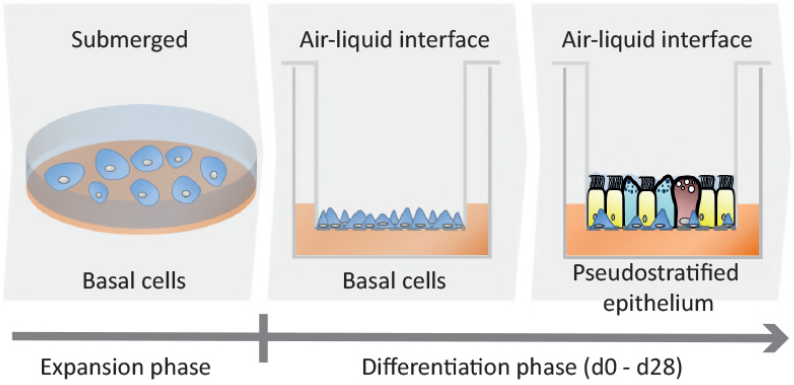

B

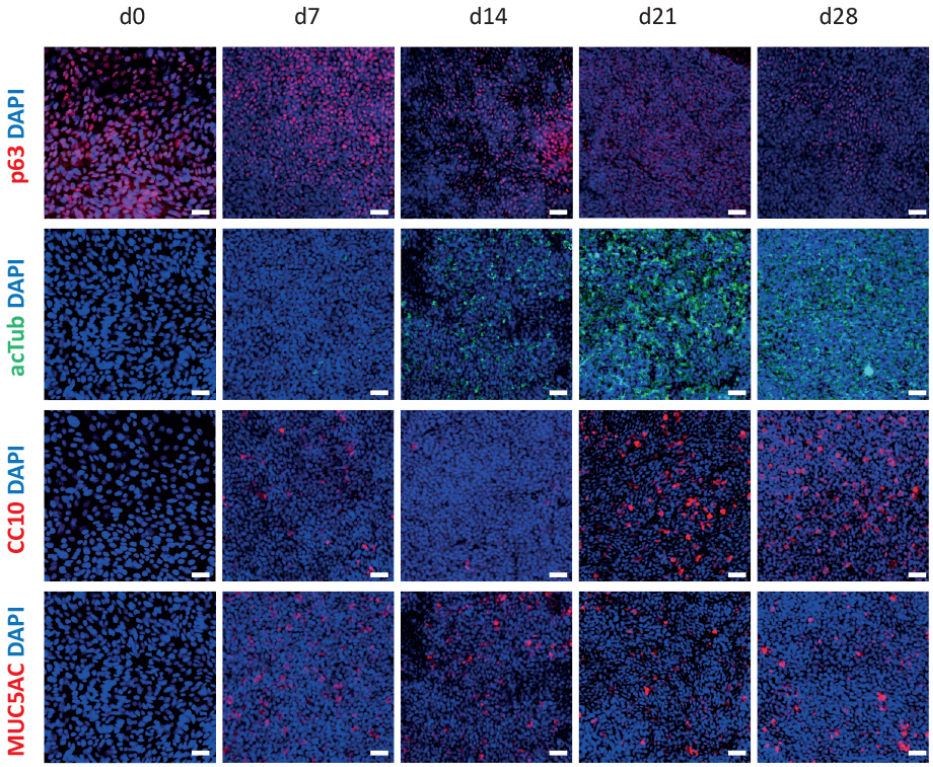

C

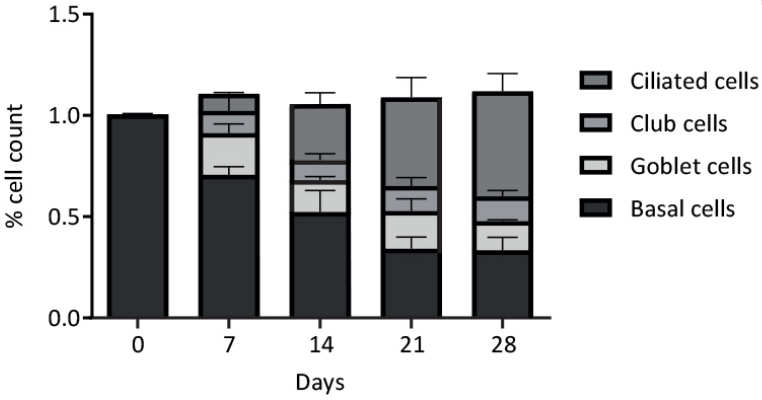

D

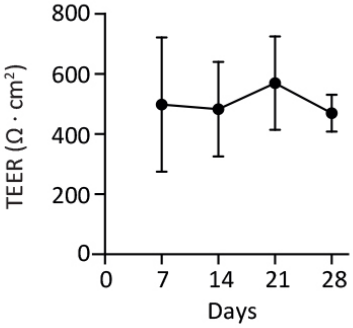

Downloaded from journals.physiology.org/journal/ajplung at Helmholtz Zentrum Muenchen (146.107.008.161) on December 16, 2021.

A

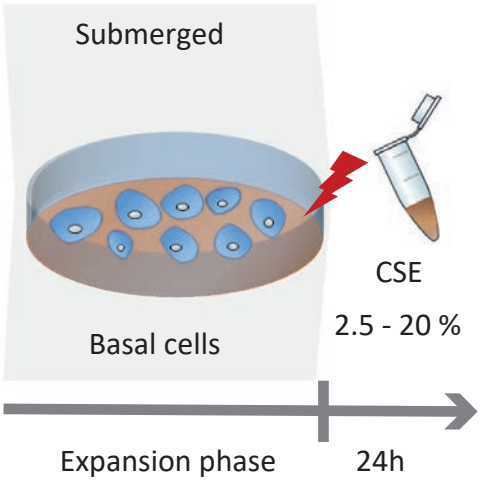

B

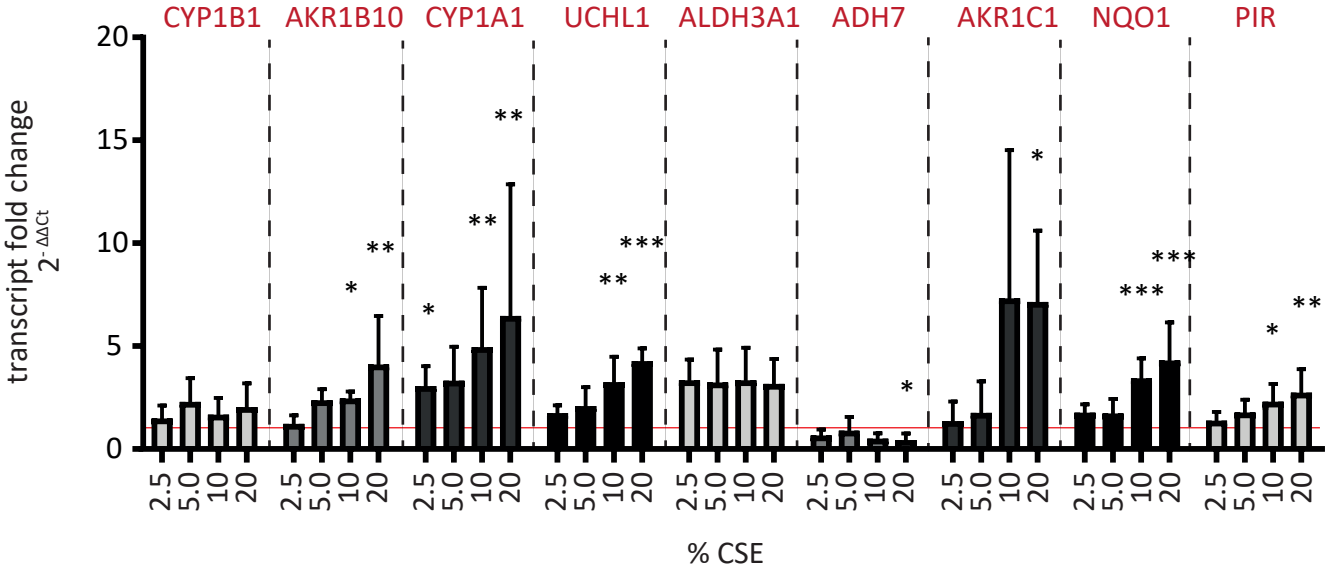

C

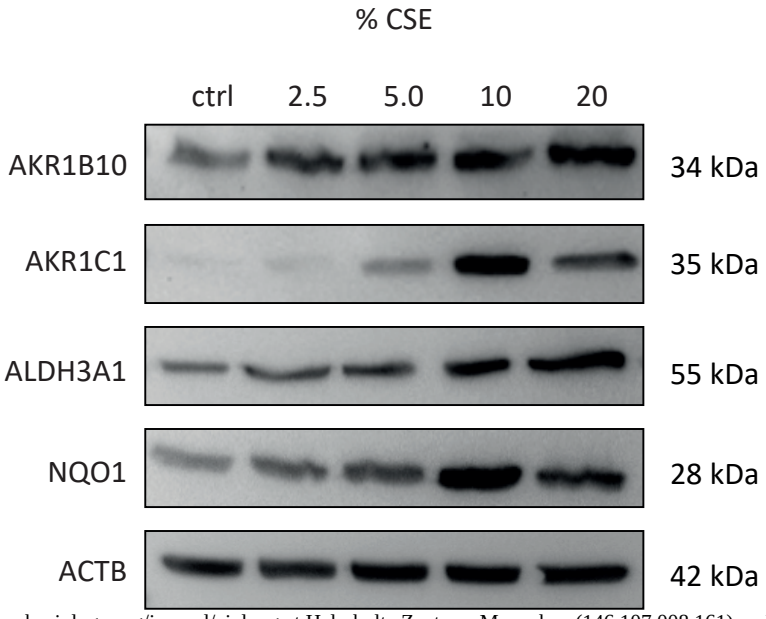

Downloaded from journals.physiology.org/journal/ajplung at Helmholtz Zentrum Muenchen (146.107.008.161) on December 16, 2021.

A

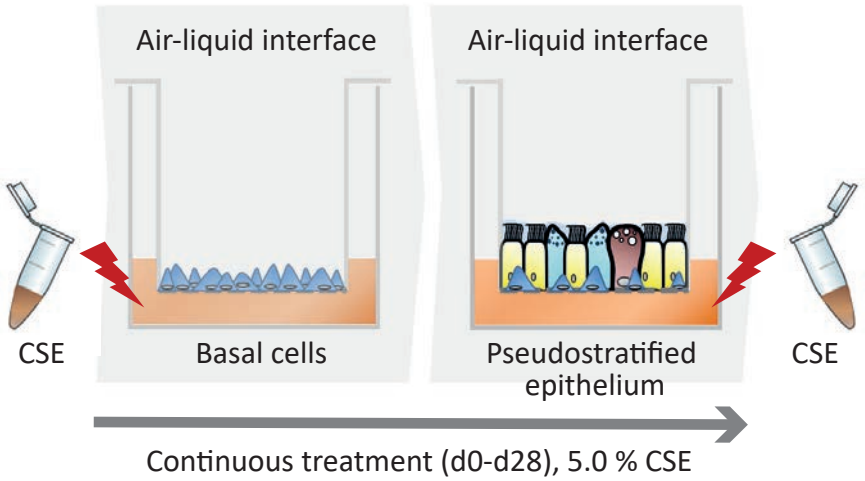

B

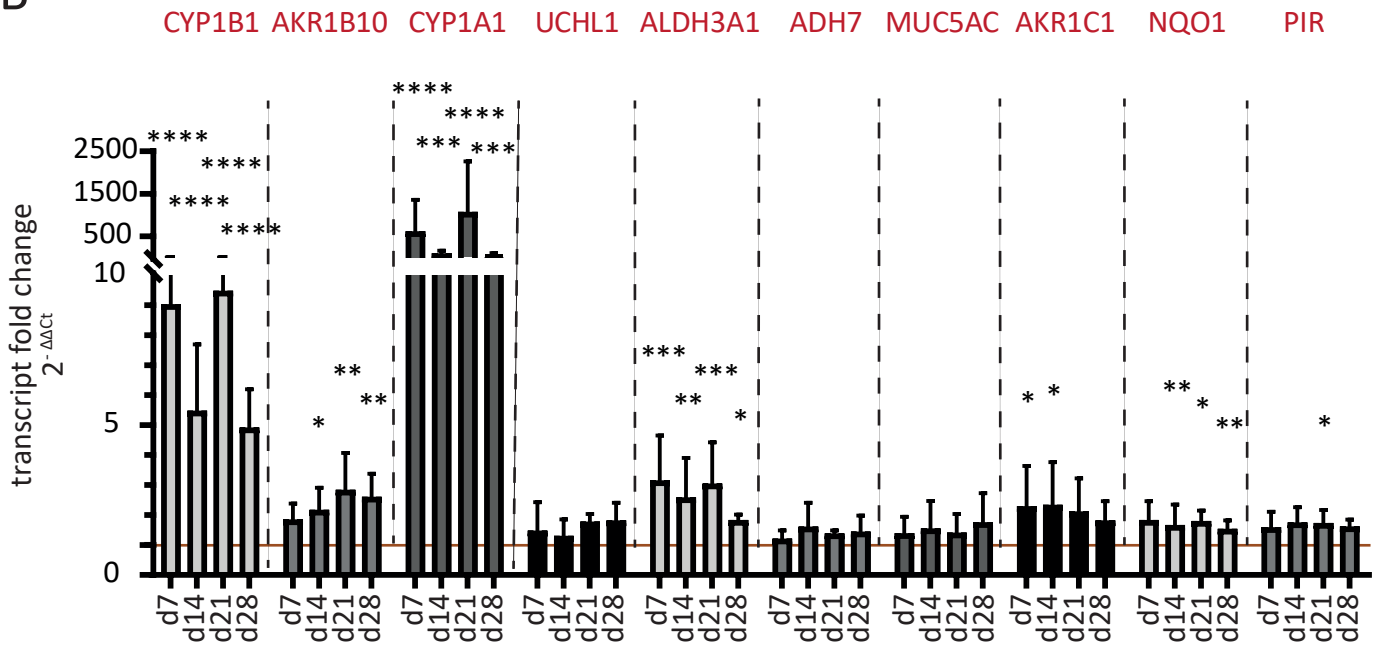

C

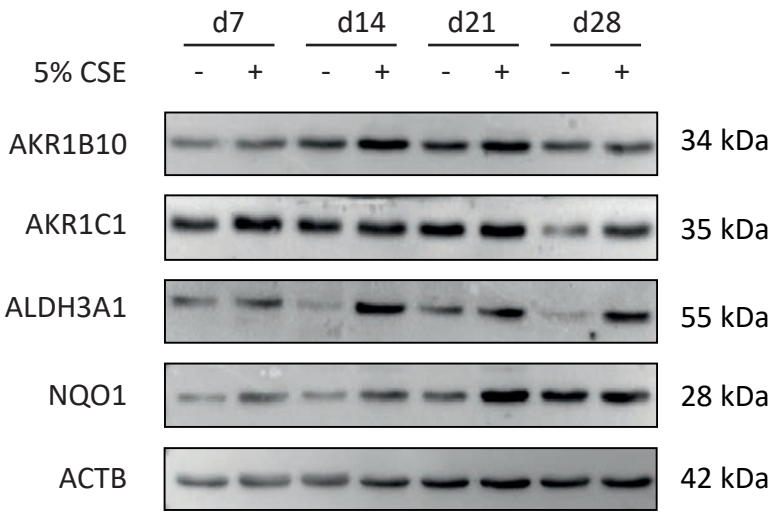

Downloaded from journals.physiology.org/journal/ajplung at Helmholtz Zentrum Muenchen (146.107.008.161) on December 16, 2021.

A

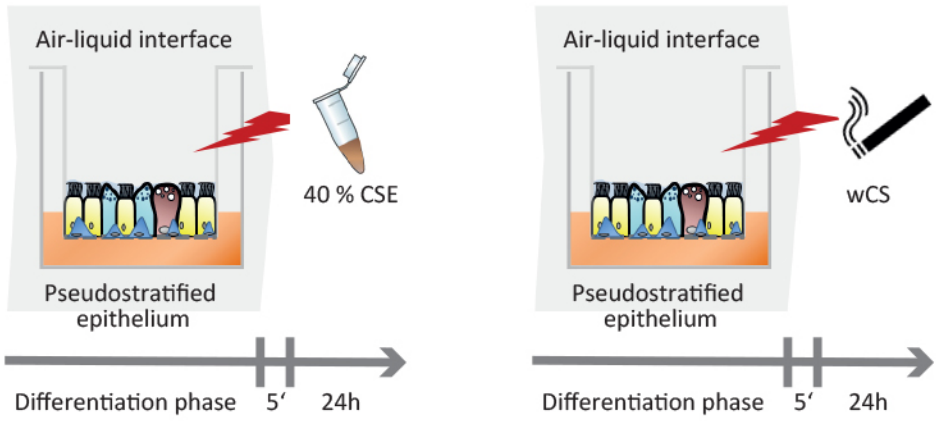

B

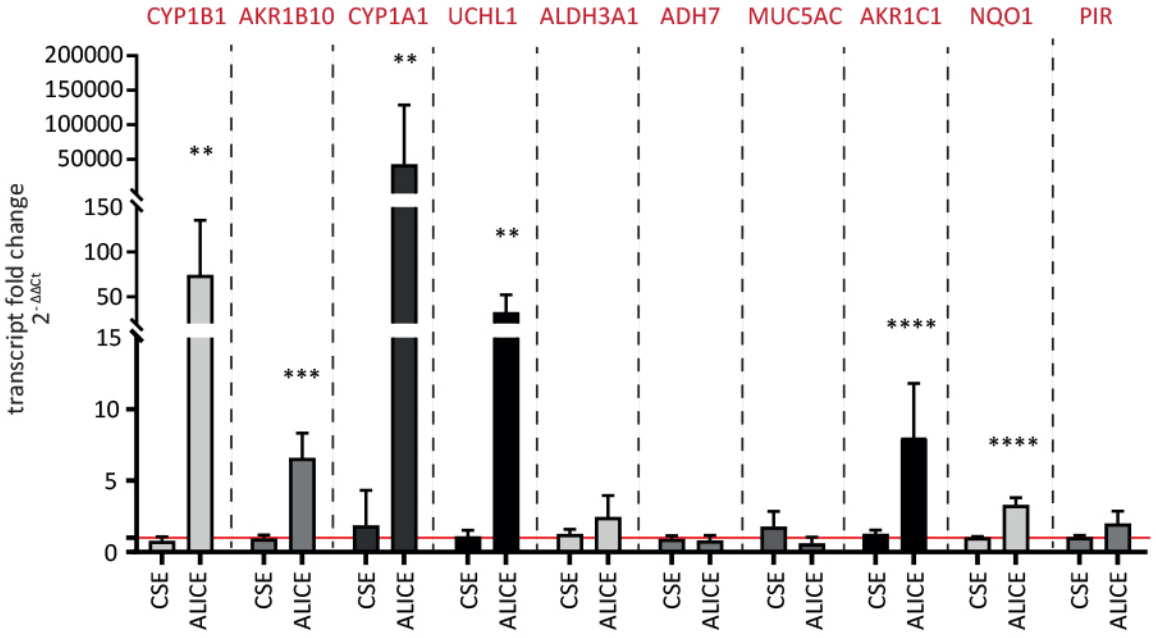

C

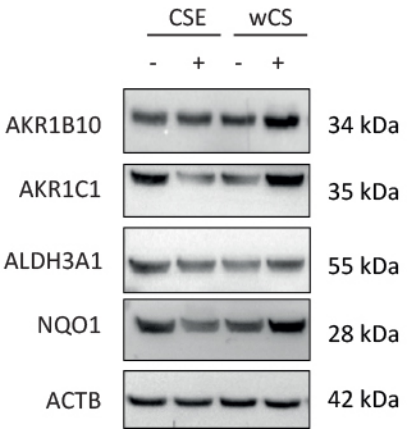

D

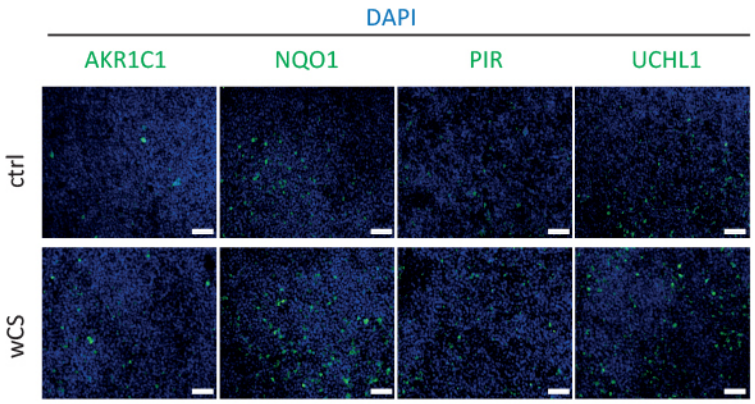

Downloaded from journals.physiology.org/journal/ajplung at Helmholtz Zentrum Muenchen (146.107.008.161) on December 16, 2021.

A

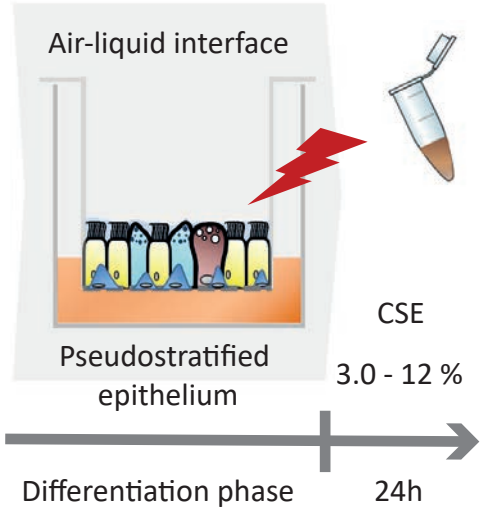

B

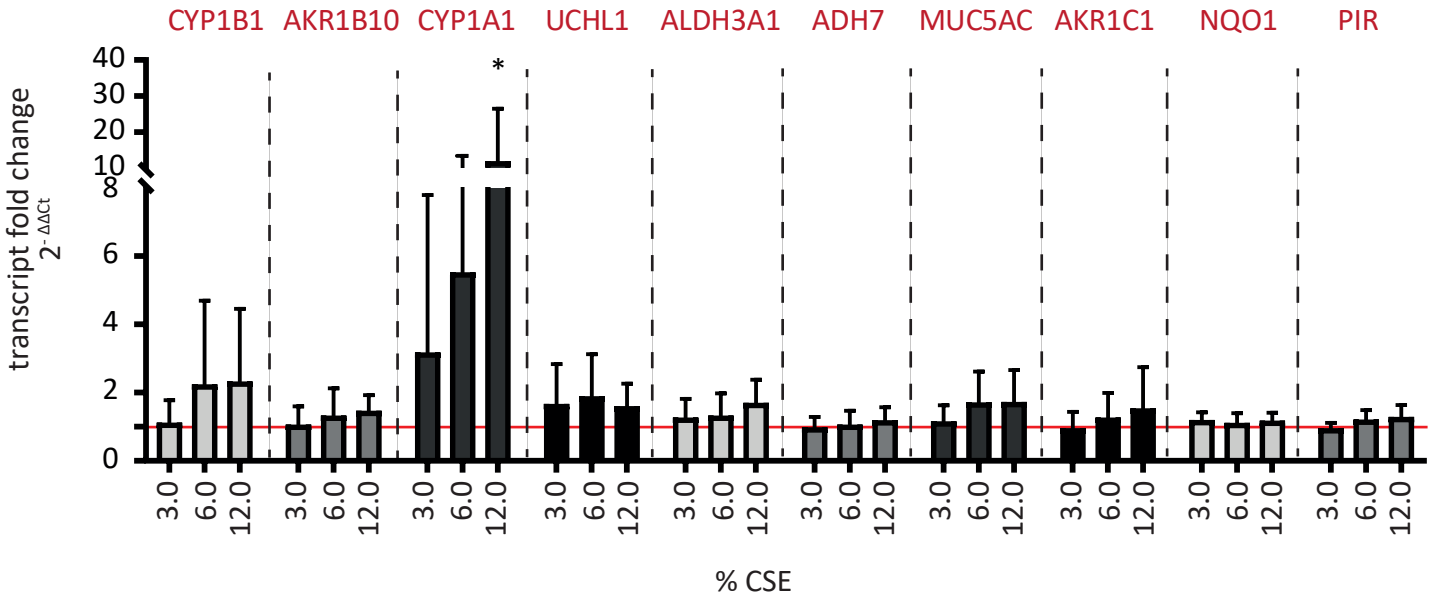

C

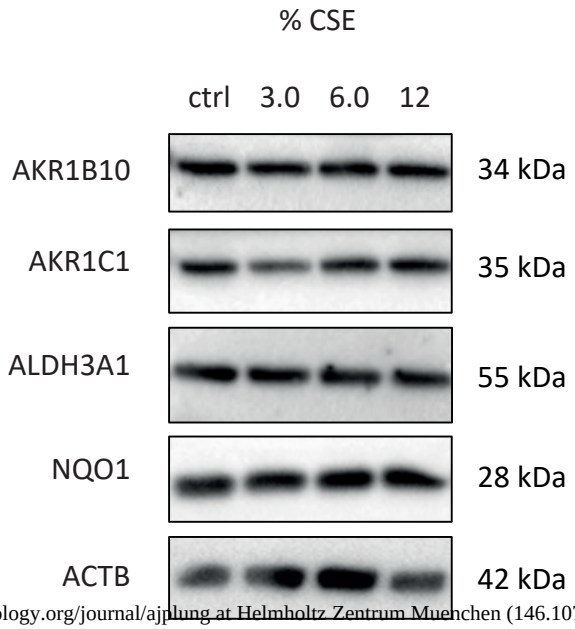

Downloaded from journals.physiology.org/journal/ajplung at Helmholtz Zentrum Muenchen (146.107.008.161) on December 16, 2021.

A

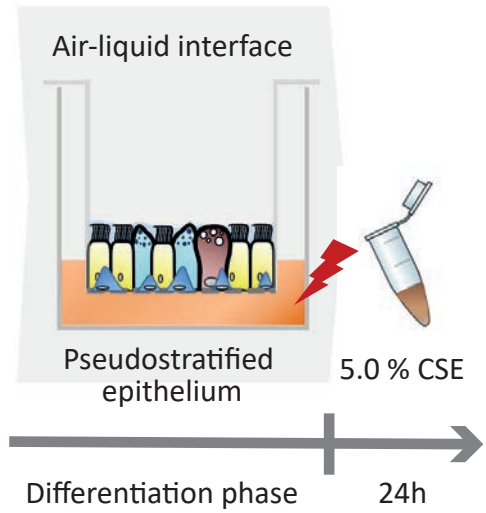

B

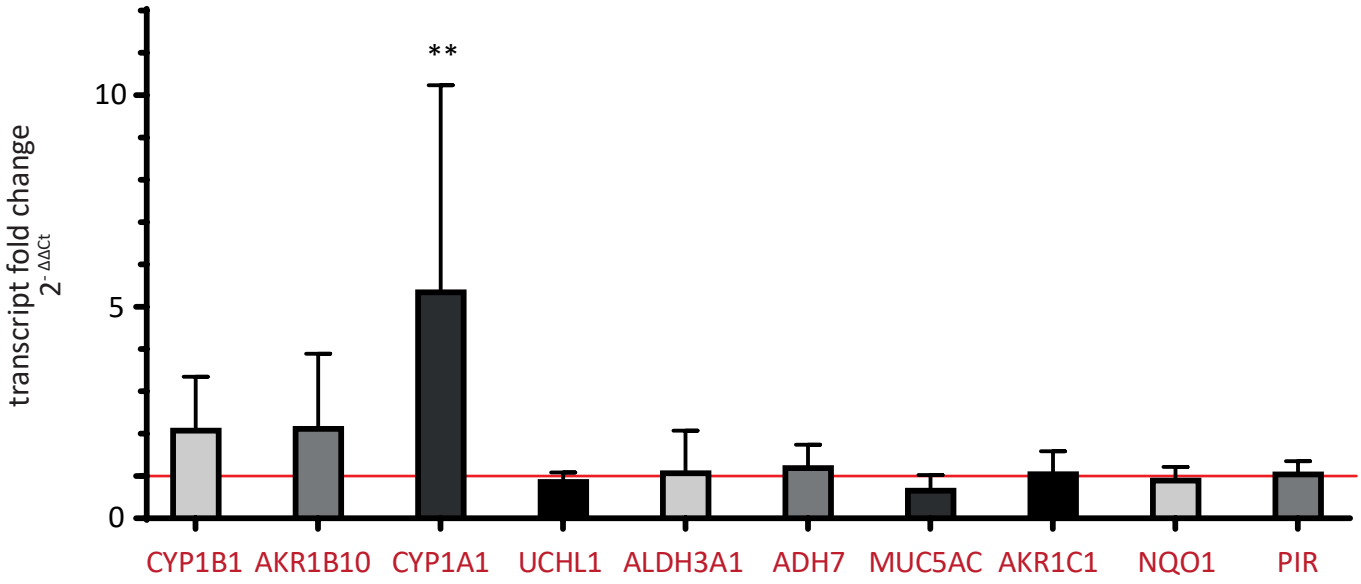

C

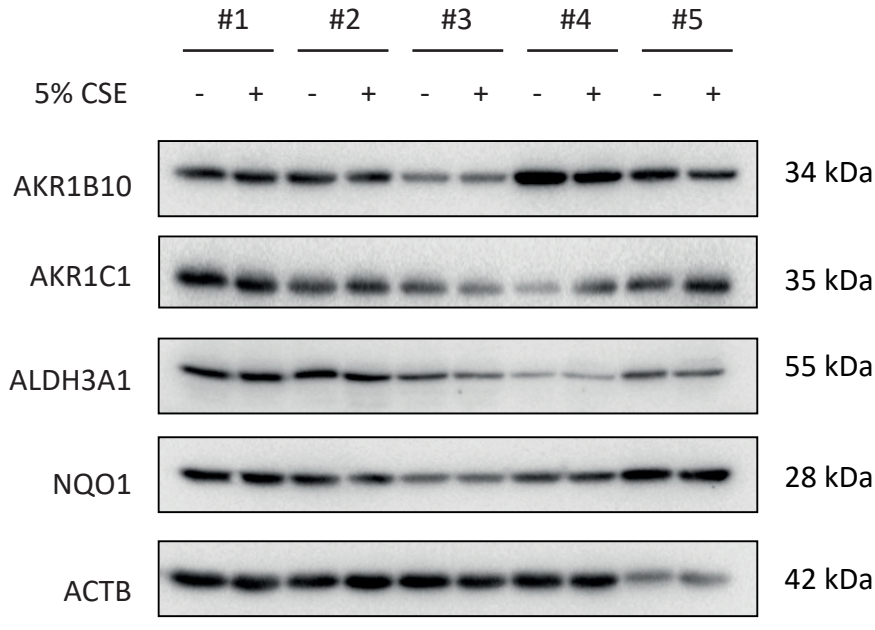

Downloaded from journals.physiology.org/journal/ajplung at Helmholtz Zentrum Muenchen (146.107.008.161) on December 16, 2021.

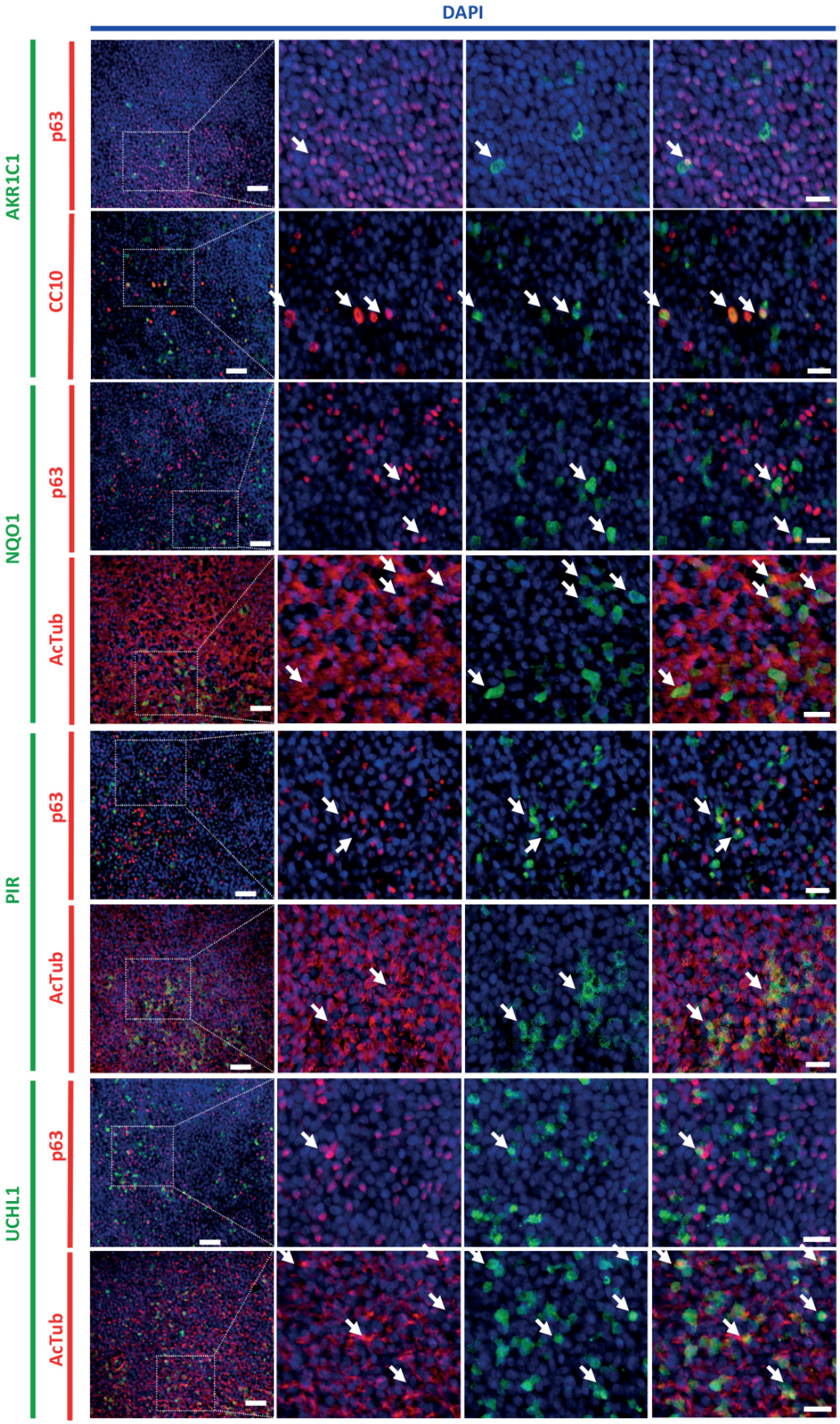

Downloaded from journals.physiology.org/journal/ajplung at Helmholtz Zentrum Muenchen (146.107.008.161) on December 16, 2021.

1

Table 1. List of genes selected as reference genes for smoke exposure based on their upregulated expression in current smokers relative to non-smokers, termed smoke exposure regulated genes (SERGs) in this study. Average fold changes are derived from microarray datasets GSE994, GSE4498, GSE7895, GSE20257 and GSE52237, and given as +/- SD.

#	Gene name	Protein	Fold change ± SD
1	**CYP1B1**	Cytochrome P450 1B1	33 ± 30
2	**AKR1B10**	Aldo-keto reductase 1B10	22 ± 3.6
3	**CYP1A1**	Cytochrome P450 1A1	13 ± 11
4	**UCHL1**	Ubiquitin carboxyl-terminal hydrolase isozyme L1	10 ± 7.2
5	**ALDH3A1**	Aldehyde dehydrogenase 3A1	7.2 ± 1.4
6	**ADH7**	Alcohol dehydrogenase class 4	5.7 ± 2.5
7	**MUC5AC**	Mucin 5AC	3.9 ± 1.3
8	**AKR1C1**	Aldo-keto reductase family 1 member C1	4.0 ± 0.7
9	**NQO1**	NAD(P)H dehydrogenase [quinone] 1	3.9 ± 0.4
10	**PIR**	Pirin	3.3 ± 0.7

2

Downloaded from journals.physiology.org/journal/ajplung at Helmholtz Zentrum Muenchen (146.107.008.161) on December 16, 2021.

Table 2. Overview of assessed cigarette smoke extract (CSE) and whole cigarette smoke (wCS) models. For details on the respective models, please refer to the relevant figures and text passages in the Material and Methods section.

#	Model	CSE concentrations	CS dose [µg/cm^2]	Volume delivered [µl/cm^2]	(Exposure) and Incubation time	Starvation	Refers to	Graphical outline
1	Acute submerged CSE exposures (n=4)	2.5%, 5%, 10%, 20%	6.6, 13, 26, 53	210	24 h	No	Figure 2	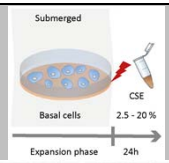
2	Chronic basolateral CSE exposure (n=5)	5%	62	890	28 days	No	Figure 3	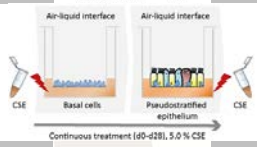
3	Short acute apical CSE exposure (n=5)	40%	100	180	(5 min) 24 h	No	Figure 4	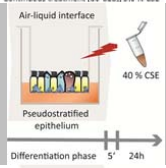
4	ALICE-Smoke (n=5)	N/A	12±1.5	N/A	(5 min) 24 h	No	Figure 4	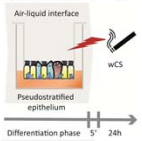
5	Acute apical exposure (n=4)	3%, 6%, 12%	7.5, 15, 30	180	24 h	Yes/No	Figure 5, S8	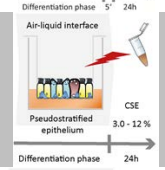
6	Acute basolateral CSE exposure (n=5)	5%	62	890	24 h	No	Figure 6	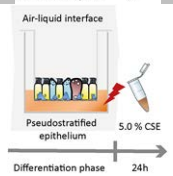

Downloaded from journals.physiology.org/journal/ajplung at Helmholtz Zentrum Muenchen (146.107.008.161) on December 16, 2021.

1

Downloaded from journals.physiology.org/journal/ajplung at Helmholtz Zentrum Muenchen (146.107.008.161) on December 16, 2021.

Table 3. Summary of SERG mRNA fold changes in the tested models, compared to upregulation by CS in current smokers (top row). Statistically significant results (p<0.05) are given in bold and the number of significantly upregulated genes is given the last column.

	Dose per area [µg/cm^2]	CYP1B1	AKR1B10	CYP1A1	UCHL1	ALDH3A1	ADH7	MUC5AC	AKR1C1	NQO1	PIR	No.
Healthy smokers[a]	**N/A**	**33**	**22**	**13**	**10**	**7.2**	**5.7**	**3.9**	**4.0**	**3.9**	**3.3**	**10**
Chronic basolateral CSE exposure[b]	**62**	**4.9**	**2.6**	**56**	1.8	**1.8**	1.4	1.7	**1.8**	**1.5**	**1.6**	**7**
ALICE-Smoke exposure	**12**	**74**	**6.6**	**42215**	**32**	2.4	0.8	0.6	**8.0**	**3.3**	2.0	**6**
Acute submerged basal cells CSE exposure[c]	**56**	2.0	**4.0**	**6.4**	**4.2**	3.1	0.4	N/A	**7.1**	**4.2**	**2.7**	**6**
Acute basolateral CSE exposure	**62**	2.1	2.2	**5.4**	0.9	1.1	1.2	0.7	1.1	0.9	1.1	**1**
Acute apical CSE exposure w/starvation[d]	**30**	1.5	1.1	**11**	1.0	1.5	1.3	1.3	1.2	1.0	1.4	**1**
Acute apical CSE exposure w/o starvation[d]	**30**	2.3	1.4	**12**	1.6	1.7	1.2	1.7	1.5	1.2	1.3	**1**
Short acute apical CSE exposure	**100**	0.8	0.9	1.8	1.1	1.2	0.9	1.8	1.2	1.0	1.0	**0**

[a] mRNA fold changes in bronchial cells brushed from healthy active smokers, obtained from transcriptomic data, references in Table 1

[b] Fold changes shown for day 28. For *CYP1A1* significance was obtained at days 7 and 21, for *AKR1C1* at days 7 and 14, and for *PIR* at day 21 (see Fig. 3)

[c] Fold changes shown for 20% CSE

[d] Fold changes shown for 12% CSE

1

Downloaded from journals.physiology.org/journal/ajplung at Helmholtz Zentrum Muenchen (146.107.008.161) on December 16, 2021.